*J. Plasma Physics* (2011), *vol.* 77, *part* 1, *pp.* 51–93.  
doi:10.1017/S0022377809990596

# Alfvén simple waves

G. M. WEBB[1], G. P. ZANK[1,2],
R. H. BURROWS[1] and R. E. RATKIEWICZ[3]

[1]CSPAR, The University of Alabama in Huntsville, Huntsville, AL 35805, USA
(gary.webb@uah.edu)

[2]Department of Physics, The University of Alabama in Huntsville,
Huntsville, AL 35899, USA

[3]Space Research Center, Bartycka 18A, 00-716 Warsaw, Poland

(Received 20 October 2009, revised 3 December 2009 and accepted 4 December 2009,
first published online 4 February 2010)

**Abstract.** Multi-dimensional Alfvén simple waves in magnetohydrodynamics (MHD) are investigated using Boillat's formalism. For simple wave solutions, all physical variables (the gas density, pressure, fluid velocity, entropy, and magnetic field induction in the MHD case) depend on a single phase function $\varphi$, which is a function of the space and time variables. The simple wave ansatz requires that the wave normal and the normal speed of the wave front depend only on the phase function $\varphi$. This leads to an implicit equation for the phase function and a generalization of the concept of a plane wave. We obtain examples of Alfvén simple waves, based on the right eigenvector solutions for the Alfvén mode. The Alfvén mode solutions have six integrals, namely that the entropy, density, magnetic pressure, and the group velocity (the sum of the Alfvén and fluid velocity) are constant throughout the wave. The eigenequations require that the rate of change of the magnetic induction $\mathbf{B}$ with $\varphi$ throughout the wave is perpendicular to both the wave normal $\mathbf{n}$ and $\mathbf{B}$. Methods to construct simple wave solutions based on specifying either a solution ansatz for $\mathbf{n}(\varphi)$ or $\mathbf{B}(\varphi)$ are developed.

## 1. Introduction

Treatments of time-dependent magnetohydrodynamics (MHD) simple waves in one Cartesian space dimension are well-established (Jeffrey and Taniuti 1964; Cabannes 1970). Webb et al. (1998) investigated multi-dimensional simple waves in gas dynamics, and gave detailed examples of multi-dimensional vortex simple waves and sound waves in two space dimensions (see also Rajee et al. 2008; Sahihi et al. 2008; Rajee and Eshraghi 2009; Nadjafikhah and Mahdipour-Shirayeh 2009 for related work).

Webb et al. (1995) studied multi-dimensional MHD simple waves using the formalism developed by Boillat (1970), in which all physical quantities of interest depend on a single phase function $\varphi(x^\alpha)$, where $\mathbf{x} = (t, x, y, z)$ are the independent time and space variables. Examples of multi-dimensional Alfvén simple waves were studied, including the two-dimensional (2D) Alfvén simple wave obtained by Barnes (1976), but no detailed analysis of the large variety of possible simple waves was carried out. Boillat's analysis shows that both the eigenvalues, or characteristic speeds $\{\lambda_i : 1 \leqslant i \leqslant n\}$ of the system of interest, and the wave normal $\mathbf{n}$ must be a function of $\varphi$. This places constraints on the functional form of $\varphi$.

The main aim of the present paper is to study in more detail multi-dimensional Alfvén simple waves. The method used by Webb et al. (1995) to construct Alfvén simple waves is developed. In this method, Gauss's law $\nabla \cdot \mathbf{B} = 0$ reduces to the equation $\mathbf{n} \cdot d\mathbf{B}/d\varphi = 0$. By specifying the functional form of the magnetic field unit vector (note $B^2$ is constant), constrains the form of the wave normal unit vector $\mathbf{n}(\varphi)$. Methods based on the Serret–Frenet moving trihedron are used in which the wave normal $\mathbf{n}(\varphi)$ is conceived as the tangent vector to a space curve $\mathbf{x} = \mathbf{X}(\varphi)$ where $\varphi$ is analogous to the distance, or affine parameter along the curve (see also Webb et al. 1998). We show that the Alfvén wave eigenequations for $\mathbf{B}$ can be rewritten as a modified form of the Serret–Frenet equations with a modified torsion coefficient to that for the curve $\mathbf{x} = \mathbf{X}(\varphi)$, with tangent vector $\mathbf{n}(\varphi)$. Using a method due to Darboux (see Eisenhart 1960), the Serret–Frenet equations are mapped onto a Ricatti equation by means of stereographic projection, which in turn is linearized by a Cole–Hopf transformation.

In Sec. 2, the MHD equations and model are introduced. In Sec. 3 Boillat's formulation of multi-dimensional simple waves is applied to the MHD equations, and the use of the Serret–Frenet frame to describe the field lines is developed. Section 4 discusses the MHD eigensystem, and in particular the eigenvectors and eigenvalues for the Alfvén mode (see also Appendix B). Section 5 gives examples of Alfvén simple waves. Section 6 concludes with a summary and discussion.

## 2. The model

The MHD equations can be written in a variety of forms. One particular form of the equations is

$$\frac{\partial \rho}{\partial t} + \nabla \cdot (\rho \mathbf{u}) = 0, \tag{2.1}$$

$$\frac{\partial}{\partial t}(\rho \mathbf{u}) + \nabla \cdot \left[ \rho \mathbf{u}\mathbf{u} + \left( p + \frac{B^2}{2\mu} \right) \mathbf{I} - \frac{\mathbf{B}\mathbf{B}}{\mu} \right] = 0, \tag{2.2}$$

$$\frac{\partial}{\partial t}(\rho S) + \nabla \cdot (\rho \mathbf{u} S) = 0, \tag{2.3}$$

$$\frac{\partial \mathbf{B}}{\partial t} - \nabla \times (\mathbf{u} \times \mathbf{B}) + \mathbf{u} \nabla \cdot \mathbf{B} = 0, \tag{2.4}$$

where $\rho$, $\mathbf{u}$, $p$, $S$, and $\mathbf{B}$ correspond to the gas density, fluid velocity, pressure, specific entropy, and magnetic induction $\mathbf{B}$ respectively, and $\mathbf{I}$ is the unit $3 \times 3$ dyadic. The gas pressure $p = p(\rho, S)$ is a function of the density $\rho$ and entropy $S$, and $\mu$ is the magnetic permeability. Equations (2.1)–(2.3) correspond to the mass, momentum and entropy conservation laws, and Faraday's equation in the MHD limit. In classical MHD, (2.1)–(2.4) are supplemented by Gauss' law:

$$\nabla \cdot \mathbf{B} = 0, \tag{2.5}$$

which implies the non-existence of magnetic monopoles.

In this paper, we consider only solutions of the MHD equations with $\nabla \cdot \mathbf{B} = 0$. There is an eigenmode of the MHD equations (2.1)–(2.4) with $\nabla \cdot \mathbf{B} \neq 0$ known as the divergence mode, which is advected with the fluid. This mode is used in eight wave Riemann solvers in numerical MHD (e.g., Powell et al. 1999; Janhunen

https://doi.org/10.1017/S0022377809990596 Published online by Cambridge University Press

2000). In this paper, we consider only the Alfvén mode solutions, which have $\nabla \cdot \mathbf{B} = 0$ (the entropy wave, and the fast and slow magnetoacoustic modes also have $\nabla \cdot \mathbf{B} = 0$).

If the equation of state for the gas is written in the form $S = f(p, \rho)$ the entropy conservation law (2.3) can alternatively be written in the form

$$\frac{\partial p}{\partial t} + \mathbf{u} \cdot \nabla p + A(p, \rho) \nabla \cdot \mathbf{u} = 0, \quad A(p, \rho) = a^2 \rho, \tag{2.6}$$

where $a^2 = \partial p / \partial \rho = -f_\rho / f_p$ is the square of the adiabatic sound speed of the gas. For the case of an ideal gas with entropy $S = C_v \ln[(p/p_1)/(\rho/\rho_1)^\gamma]$, where $\gamma = C_p / C_v$ is the ratio of specific heats at constant pressure and volume respectively, $A(p, \rho) = \gamma p$ in (2.6). An alternative formulation uses the internal energy density relation $\varepsilon = \varepsilon(\rho, S)$ as the equation of state for the gas, in which case $p = \rho \partial \varepsilon / \partial \rho - \varepsilon$ and $\rho T = \partial \varepsilon / \partial S$ define the pressure and temperature of the gas. For an ideal gas with adiabatic index $\gamma$, $\varepsilon = p/(\gamma - 1)$. Equation (2.3) is also equivalent to the entropy advection equation:

$$\frac{\partial S}{\partial t} + \mathbf{u} \cdot \nabla S = 0. \tag{2.7}$$

Equations (2.3), (2.6) and (2.7) are all equivalent to the comoving energy equation for the gas.

*Comment 1:*

In numerical MHD, Powell et al. (1999) and Janhunen (2000) developed eight wave Riemann solvers that include the $\mathbf{u} \nabla \cdot \mathbf{B}$ term in Faradays' equation (2.4). Taking the divergence of (2.4) gives the continuity equation:

$$\frac{\partial}{\partial t}(\nabla \cdot \mathbf{B}) + \nabla \cdot (\mathbf{u} \nabla \cdot \mathbf{B}) = 0. \tag{2.8}$$

The numerically generated $\nabla \cdot \mathbf{B} \neq 0$ in these methods is advected with the fluid, thus preventing accumulation of $\nabla \cdot \mathbf{B} \neq 0$ in the internal numerical domain. The eigenmode with $\nabla \cdot \mathbf{B} \neq 0$ which is advected with the flow in (2.8) is referred to as the divergence wave (see Webb et al. 2009 for an exact simple wave solution for the divergence wave eigenmode and further discussion of this issue).

The total energy equation for the system (2.1)–(2.4),

$$\frac{\partial}{\partial t}\left(\frac{1}{2}\rho u^2 + \varepsilon + \frac{B^2}{2\mu}\right) + \nabla \cdot \left[\mathbf{u}\left(\varepsilon + p + \frac{1}{2}\rho |\mathbf{u}|^2\right) + \frac{\mathbf{E} \times \mathbf{B}}{\mu}\right] = 0, \tag{2.9}$$

follows from adding together: (i) the electromagnetic energy equation:

$$\frac{\partial}{\partial t}\left(\frac{B^2}{2\mu}\right) + \nabla \cdot \left(\frac{\mathbf{E} \times \mathbf{B}}{\mu}\right) = -\mathbf{J} \cdot \mathbf{E} - \mathbf{u} \cdot \mathbf{B} \frac{\nabla \cdot \mathbf{B}}{\mu}, \tag{2.10}$$

where $\mathbf{S} = \mathbf{E} \times \mathbf{B}/\mu$ is the Poynting flux, $\mathbf{E} = -\mathbf{u} \times \mathbf{B}$ is the motional electric field, and $\mathbf{J} = \nabla \times \mathbf{B}/\mu$ is Ampere's law for the electric current in the MHD limit; (ii) the comoving gas energy equation:

$$\frac{\partial \varepsilon}{\partial t} + \nabla \cdot [\mathbf{u}(\varepsilon + p)] = \mathbf{u} \cdot \nabla p; \tag{2.11}$$

and (iii) the gas kinetic energy equation:

$$\frac{\partial}{\partial t}\left(\frac{1}{2}\rho u^2\right) + \nabla \cdot \left(\mathbf{u} \frac{1}{2}\rho u^2\right) = -\mathbf{u} \cdot \nabla p + \mathbf{J} \cdot \mathbf{E} + \mathbf{u} \cdot \mathbf{B} \frac{\nabla \cdot \mathbf{B}}{\mu}, \tag{2.12}$$

https://doi.org/10.1017/S0022377809990596 Published online by Cambridge University Press

*Comment* 2:

Poynting's theorem (2.10) follows from taking the scalar product of Faraday's equation (2.4) with **B**.

*Comment 3:*

The comoving gas energy equation (2.11) follows from the second law of thermodynamics: $dQ = TdS = dU + pd\tau$, where $U = \varepsilon/\rho$ is the internal energy per unit mass of the gas, $\tau = 1/\rho$ is the specific volume, and by noting that $dS/dt = 0$ for an adiabatic process, where $d/dt = \partial/\partial t + \mathbf{u}\cdot\nabla$, is the Lagrangian time derivative following the flow.

*Comment 4:*

The kinetic energy equation (2.12) for the gas follows from the momentum equation (2.2), which with the aid of the continuity equation (2.1) can be cast in the form:

$$\rho\left(\frac{\partial \mathbf{u}}{\partial t} + \mathbf{u}\cdot\nabla\mathbf{u}\right) = -\nabla p + \mathbf{J}\times\mathbf{B} + \mathbf{B}\frac{\nabla\cdot\mathbf{B}}{\mu}, \tag{2.13}$$

where $\mathbf{J} = \nabla\times\mathbf{B}/\mu$ is the current. Taking the scalar product of (2.13) with **u** and using the continuity equation (2.1) gives the gas kinetic energy equation (2.12).

## 3. The simple wave formalism

Following the development of Boillat (1970), the MHD equations are first written in the matrix form

$$\mathbf{A}^{(\alpha)}\frac{\partial \mathbf{W}}{\partial x^{\alpha}} = 0, \tag{3.1}$$

where

$$\mathbf{W} = (\rho, u_x, u_y, u_z, B_x, B_y, B_z, p)^T \tag{3.2}$$

is the state vector of the system using the primitive variables The matrix $\mathbf{A}^{(0)}$ is the unit $8\times 8$ identity matrix, and we use the notation $(x^0, x^1, x^2, x^3) = (t, x, y, z)$ to denote the independent variables. The detailed form of the matrices $A^{(i)}$ for the conservative Janhunen (2000) equation system based on (2.1)–(2.4) are given in appendix A.

### *3.1. Boillat's solution ansatz*

In Boillat's method, one searches for solutions of the MHD equations (3.1) of the form

$$\mathbf{W} = \mathbf{W}(\varphi), \tag{3.3}$$

where $\varphi(t, x, y, z)$ is the wave phase. The equations

$$\omega = -\varphi_t, \quad \mathbf{k} = \nabla\varphi, \quad \lambda = \frac{\omega}{k} = -\frac{\varphi_t}{|\nabla\varphi|}, \quad \mathbf{n} = \frac{\nabla\varphi}{|\nabla\varphi|}, \tag{3.4}$$

locally define the wave frequency $\omega$, wave number **k**, and wave phase speed $\lambda$ parallel to the wave normal **n**. Substitution of the solution ansatz (3.3) in the MHD equations (3.1) yields the matrix equation

$$[\mathbf{A}_n - \lambda\mathbf{I}]\cdot\frac{d\mathbf{W}}{d\varphi} = 0, \tag{3.5}$$

where

$$\mathbf{A}_n = \mathbf{A}^{(1)}n_x + \mathbf{A}^{(2)}n_y + \mathbf{A}^{(3)}n_z. \tag{3.6}$$

https://doi.org/10.1017/S0022377809990596 Published online by Cambridge University Press

The general solution of the eigenequation (3.5) corresponding to the $k$th eigenmode is of the form

$$\frac{d\mathbf{W}}{d\varphi} = a_k(\varphi)\mathbf{R}_k, \tag{3.7}$$

where $a_k$ determines the wave amplitude and $\mathbf{R}_k$ is the right eigenvector of the matrix $\mathbf{A}_n$ corresponding to the $k$th wave mode. For the case where two or more of the eigenvalues are coincident, the solution (3.7) may be written as a sum over the corresponding wave modes. Boillat (1970) noted that if the solution for $\mathbf{W}$ is to be solely a function of $\varphi$, it is necessary $\mathbf{n}$ and $\lambda(\mathbf{W}, \mathbf{n})$ are functions only of $\varphi$. This places constraints on the possible functional form of $\varphi(t, x, y, z)$, which we discuss below.

The requirements that $\lambda = \lambda(\varphi)$ and $\mathbf{n} = \mathbf{n}(\varphi)$ imply that $\varphi$ must satisfy the first-order partial differential equations

$$\mathbf{n}(\varphi) = \frac{\nabla\varphi}{|\nabla\varphi|}, \quad \lambda(\varphi) = -\frac{\varphi_t}{|\nabla\varphi|} \tag{3.8}$$

for the eigenmode of interest. Boillat showed that the general solution of the differential equations (3.8) for $\varphi$ is of the form

$$f(\varphi) = \mathbf{r} \cdot \mathbf{n}(\varphi) - \lambda(\varphi)t, \tag{3.9}$$

where $\mathbf{r} = (x, y, z)$, and $f(\varphi)$ is an arbitrary differentiable function of $\varphi$. For non-exceptional waves with $d\lambda/d\varphi \neq 0$, centered simple waves correspond to the choice $f(\varphi) = 0$, and non-centered simple wave to $f(\varphi) \neq 0$.

Implicit differentiation of (3.9) with respect to $(t, x, y, z)$ yields the derivatives of $\varphi$:

$$\varphi_t = -\frac{\lambda}{F}, \quad \nabla\varphi = \frac{\mathbf{n}(\varphi)}{F}, \tag{3.10}$$

where

$$F = f'(\varphi) + \frac{d\lambda}{d\varphi}t - \mathbf{r}\cdot\frac{d\mathbf{n}}{d\varphi} = \frac{1}{|\nabla\varphi|}. \tag{3.11}$$

Note that for a consistent solution $F$ must be positive. At points where $F \to 0$, $|\nabla\varphi| \to \infty$; $|\nabla W^\alpha| \to \infty$ and $|W_t^\alpha| \to \infty$, and wave breaking occurs.

Since $\lambda = \lambda(\mathbf{W}, \mathbf{n})$, the group velocity of the wave is given by

$$\mathbf{V}_g = \frac{\partial\omega}{\partial\mathbf{k}} = \lambda\mathbf{n} + (\mathbf{I} - \mathbf{nn}) \cdot \nabla_{\mathbf{n}}\lambda. \tag{3.12}$$

Using (3.12) it follows that $\mathbf{W}(\varphi)$ does not change along the ray path:

$$\frac{\partial\mathbf{W}}{\partial t} + \mathbf{V}_g \cdot \nabla\mathbf{W} = 0. \tag{3.13}$$

For exceptional waves in which $d\lambda/d\varphi = 0$ one finds (Boillat 1970)

$$\nabla \cdot \mathbf{V}_g = 0. \tag{3.14}$$

It is worth noting that (3.9), for a fixed parameter $\varphi$, consists of a family of planes in $(t, x, y, z)$ space, i.e.,

$$G = f(\varphi) + \lambda(\varphi)t - xn^x(\varphi) - yn^y(\varphi) - zn^z(\varphi) = 0. \tag{3.15}$$

https://doi.org/10.1017/S0022377809990596 Published online by Cambridge University Press

The *characteristic curve* of the family of planes (3.15) is obtained by solving the equations

$$G(x,y,z,t,\varphi)=0 \quad \text{and} \quad G_\varphi(x,y,z,t,\varphi)=0, \tag{3.16}$$

simultaneously for a fixed $\varphi$ (e.g., Sneddon 1957, Appendix). Evaluating $G_\varphi$ in (3.16) we obtain:

$$G_\varphi = F = f'(\varphi) + \frac{d\lambda}{d\varphi}t - \mathbf{r}\cdot\frac{d\mathbf{n}}{d\varphi} = \frac{1}{|\nabla\varphi|}. \tag{3.17}$$

The family of characteristic curves obtained for all allowable $\varphi$ obtained by eliminating $\varphi$ in (3.16) defines the *envelope* of the family of planes (3.15). From (3.10)–(3.11) we note that the wave breaks on the envelope of the family of planes (3.15). The family of planes (3.15) consists of *straight lines* and hence is a *ruled surface*, and the envelope obtained by solving (3.16) is a *developable surface* (Sneddon 1957). The theory of ruled surfaces has a rich structure depending on the arbitrary functions of $\varphi$ occurring in (3.9) (e.g., the edge of regression obtained by solving $G=0$, $G_\varphi=0$ and $G_{\varphi\varphi}=0$ is also of geometrical interest), but the above discussion is sufficient for our present purposes.

### *3.2. Magnetic field line and streamline equations*

The simple wave ansatz, considered by Boillat (1970), has implications for the geometry of the magnetic field line

$$\frac{dx}{B_x(\varphi)} = \frac{dy}{B_y(\varphi)} = \frac{dz}{B_z(\varphi)}, \tag{3.18}$$

and fluid streamline

$$\frac{dx}{u_x(\varphi)} = \frac{dy}{u_y(\varphi)} = \frac{dz}{u_z(\varphi)}, \tag{3.19}$$

differential equations associated with simple waves. The form of the field line equations (3.18) suggests that the wave phase is a natural parameter associated with the family of integral curves for (3.18) and (3.19).

The solution ansatz (3.9) for the wave phase $\varphi$ depends on the functional form assumed for the wave normal $\mathbf{n}(\varphi)$, and the geometry of the field lines is clearly related to the geometry of the curve $C$ with tangent vector $\mathbf{n}(\varphi)$ on the unit sphere. We think of $\mathbf{n}(\varphi)$ as the tangent vector to a curve $\mathbf{X}(\varphi)$ with unit tangent vector

$$\mathbf{d}_1 = \mathbf{T}(\varphi) = \frac{\mathbf{X}'(\varphi)}{|\mathbf{X}'(\varphi)|}. \tag{3.20}$$

If the curve $\mathbf{X}(\varphi)$ is three times differentiable, then the geometry of the curve is conveniently described by the use of the Serret–Frenet formulae (e.g., Lipschutz 1969, Ch. 5). If $\mathbf{X}(\varphi)$ is not thrice differentiable one can introduce a general director basis $(\mathbf{d}_1,\mathbf{d}_2,\mathbf{d}_3)$ to frame the curve (e.g., Bishop 1975; Goriely and Tabor 1997; Webb et al. 1998). The unit vectors $\mathbf{d}_2$ and $\mathbf{d}_3$ are two differentiable functions spanning the normal plane in such a way that $\{\mathbf{d}_1,\mathbf{d}_2,\mathbf{d}_3\}$ form a right-handed orthonormal triad ($\mathbf{d}_1\times\mathbf{d}_2=\mathbf{d}_3$, $\mathbf{d}_2\times\mathbf{d}_3=\mathbf{d}_1$). The choice of the vectors $\mathbf{d}_2$ and $\mathbf{d}_3$ is arbitrary as long as they span the normal plane. From the orthonormality conditions $\mathbf{d}_i\cdot\mathbf{d}_j=\delta_{ij}$ it follows that

$$\mathbf{d}_i' = \sum_{k=1}^{3} K_{ik}\mathbf{d}_k = \kappa\times\mathbf{d_i}, \tag{3.21}$$

https://doi.org/10.1017/S0022377809990596 Published online by Cambridge University Press

where $\kappa = \sum_{i=1}^{3} \kappa_i \mathbf{d}_i$ is the twist vector. Note that $\mathbf{K}_{ij} = \mathbf{d}_i' \cdot \mathbf{d}_j = \kappa_s \epsilon_{sij}$ is given by

$$\mathbf{K} = \begin{pmatrix} 0 & \kappa_3 & -\kappa_2 \\ -\kappa_3 & 0 & \kappa_1 \\ \kappa_2 & -\kappa_1 & 0 \end{pmatrix}. \tag{3.22}$$

For the special case for the Serret–Frenet frame basis,

$$\mathbf{e}_1 = \mathbf{n}(\varphi), \quad \mathbf{e}_2 = \frac{\mathbf{n}'(\varphi)}{|\mathbf{n}'(\varphi)|}, \quad \mathbf{e}_3 = \mathbf{e}_1 \times \mathbf{e}_2, \tag{3.23}$$

the Serret–Frenet equations describing the geometry of the curve $C$ (e.g., Lipschutz 1969, Ch. 5) are

$$\frac{d\mathbf{e}_1}{d\varphi} = \kappa \mathbf{e}_2, \quad \frac{d\mathbf{e}_2}{d\varphi} = -\kappa \mathbf{e}_1 + \tau \mathbf{e}_3, \quad \frac{d\mathbf{e}_3}{d\varphi} = -\tau \mathbf{e}_2, \tag{3.24}$$

where $\kappa(\varphi)$ and $\tau(\varphi)$ are the curvature and torsion coefficients of the curve. In this case, the components of the twist vector are

$$\kappa_1 = \tau, \quad \kappa_2 = 0, \quad \kappa_3 = \kappa. \tag{3.25}$$

*Comment*

In (3.24) and (3.25) we use $\varphi$ as the parameter along the curve $\mathbf{X}(\varphi)$. If instead we had used the natural parameter $s$ (distance along the curve), then the natural curvature and torsion coefficients are $\bar{\kappa}(s) = \kappa(\varphi)/s'(\varphi)$ and $\bar{\tau}(s) = \tau(\varphi)/s'(\varphi)$. In the present application of the Serret–Frenet formalism, it is more natural to use the wave phase $\varphi$ as the parameter along the curve. It is a simple matter in applications to convert to the natural curvature and torsion coefficients $\bar{\kappa}(s)$ and $\bar{\tau}(s)$, if desired. Note that $s'(\varphi) = (x_\varphi^2 + y_\varphi^2 + z_\varphi^2)^{1/2}$, where $\mathbf{X}(\varphi) = (x(\varphi), y(\varphi), z(\varphi))$.

To obtain a convenient form of the field line equations (3.18) in the group velocity frame, we introduce generalized coordinates:

$$\tilde{q}_j = \tilde{\mathbf{r}} \cdot \mathbf{d}_j, \quad \tilde{\mathbf{r}} = \mathbf{r} - \mathbf{V}_g t, \quad j = 1, 2, 3, \tag{3.26}$$

where $\mathbf{V}_g(\varphi)$ is the group velocity (3.12). From (3.9) and (3.12),

$$\tilde{q}_1 = \tilde{\mathbf{r}} \cdot \mathbf{n}(\varphi) = f(\varphi). \tag{3.27}$$

The gradients of the $\tilde{q}_j$ with respect to $\mathbf{r}$ are

$$\begin{aligned} \nabla \tilde{q}_1 &= \frac{f'(\varphi)\mathbf{d}_1}{F}, \\ \nabla \tilde{q}_2 &= \mathbf{d}_2 + \frac{\mathbf{d}_1}{F}(\kappa_1 \tilde{q}_3 - \kappa_3 \tilde{q}_1 - \mathbf{d}_2 \cdot \mathbf{V}_g'(\varphi)t), \\ \nabla \tilde{q}_3 &= \mathbf{d}_3 + \frac{\mathbf{d}_1}{F}(\kappa_2 \tilde{q}_1 - \kappa_1 \tilde{q}_2 - \mathbf{d}_3 \cdot \mathbf{V}_g'(\varphi)t), \end{aligned} \tag{3.28}$$

where

$$F = f'(\varphi) + \kappa_2 \tilde{q}_3 - \kappa_3 \tilde{q}_2 + \mathbf{d}_1 \cdot \mathbf{V}_g'(\varphi)t \tag{3.29}$$

is the function $F = 1/|\nabla\varphi|$ defined in (3.11).

https://doi.org/10.1017/S0022377809990596 Published online by Cambridge University Press

Using (3.27)–(3.29) the field line equations $d\mathbf{r} = \alpha\mathbf{B}$ in (3.18) can be expressed in the form

$$\alpha = \frac{Fd\varphi}{B_1} = \frac{Fd\tilde{q}_2}{FB_2 + B_1(\kappa_1\tilde{q}_3 - \kappa_3\tilde{q}_1 - \mathbf{d}_2\cdot\mathbf{V}_g'(\varphi)t)},$$

$$= \frac{Fd\tilde{q}_3}{FB_3 + B_1(\kappa_2\tilde{q}_1 - \kappa_1\tilde{q}_2 - \mathbf{d}_3\cdot\mathbf{V}_g'(\varphi)t)}. \tag{3.30}$$

Note that we use $d\varphi$ rather than $d\tilde{q}_1$ in (3.30) since $f(\varphi) = 0$ in a centred simple wave. It is also necessary for $\mathbf{n}(\varphi)$ to have continuous derivatives for the formulation (3.30) to make sense. For the case where $\mathbf{n}(\varphi)$ is a constant unit vector, equations (3.30) are not applicable, and it is then necessary to use the original form of the field line equations (3.18). The Jacobian

$$J = \frac{\partial(\varphi, \tilde{q}_2, \tilde{q}_3)}{\partial(x, y, z)} = \nabla\varphi\cdot\nabla\tilde{q}_2\times\nabla\tilde{q}_3 = \frac{1}{F}. \tag{3.31}$$

Thus, the Jacobian of the transformation between the new variables $\{\varphi, \tilde{q}_2, \tilde{q}_3\}$ and $\{x, y, z\}$ is in general non-zero and well defined, but $J \to \infty$ on the wave envelope where $F \to 0$ and $|\nabla\varphi| \to \infty$. Hence the use of $\varphi$, $\tilde{q}_2$, and $\tilde{q}_3$ as independent variables is valid off the wave envelope where $F \neq 0$.

*Comment*: 1

The field line equations can also be expressed in the forms

$$\frac{d\mathbf{x}}{d\varphi} = F\frac{\mathbf{B}}{B_1} \quad \text{or} \quad \frac{d\tilde{\mathbf{x}}}{d\varphi} = F\frac{\mathbf{B}}{B_1} - \mathbf{V}_g'(\varphi)t. \tag{3.32}$$

To prove (3.32), note that for constant $t$,

$$d\varphi = \nabla\varphi\cdot d\mathbf{x} = \frac{\mathbf{n}\cdot d\mathbf{x}}{F}. \tag{3.33}$$

The field line equations (3.18) have the form

$$d\mathbf{x} = \alpha\mathbf{B} \quad \text{where} \quad d\mathbf{x}\cdot\mathbf{n} = \alpha B_1. \tag{3.34}$$

From (3.33) and (3.34) it follows that

$$\alpha = \frac{d\mathbf{x}\cdot\mathbf{n}}{B_1} = \frac{Fd\varphi}{B_1}. \tag{3.35}$$

Combining (3.34) and (3.35) gives the first form of the field line equations in (3.32). The second form of the field lines in (3.32) follows by noting that $\tilde{\mathbf{x}} = \mathbf{x} - \mathbf{V}_g(\varphi)t$ is the position vector in the group velocity frame. For simple Alfvén waves the group velocity $\mathbf{V}_g(\varphi) = (V_1, V_1, V_3)$ is a constant vector and the field lines in the group velocity frame are $d\tilde{\mathbf{x}}/d\varphi = F\mathbf{B}/B_1$.

*Comment* 2:

From (3.32) the tangent vector to the field lines $d\mathbf{x}/d\varphi = 0$ on the wave envelope where $F = 0$, provided, $B_1$ is non-zero on the envelope. This implies that, in general, the field lines form a cusp at the points where the field lines intersect the wave envelope. This property of the field lines is verified in the simple Alfvén wave solutions presented in Sec. 5.

*Comment*: 3

If we had used arc length $s$ along the magnetic field line, rather than $\varphi$, then the field line equations (3.32) would read $d\mathbf{x}/ds = \mathbf{B}/B$, where $s'(\varphi) = FB/B_1$.

https://doi.org/10.1017/S0022377809990596 Published online by Cambridge University Press

*Comment* 4:

The field line equations (3.32) could also be analyzed using the Serret–Frenet formalism, with curvature and torsion coefficients $\kappa_B$ and $\tau_B$, but this will not be done here.

### *3.3. Serret–Frenet base formulae*

Some basic formulae using the Serret–Frenet base are listed below. Using the Serret–Frenet formulae (3.24), we obtain

$$\frac{d\mathbf{B}}{d\varphi} = \left(\frac{dB_1}{d\varphi} - \kappa B_2\right)\mathbf{e}_1 + \left(\frac{dB_2}{d\varphi} + \kappa B_1 - \tau B_3\right)\mathbf{e}_2 + \left(\frac{dB_3}{d\varphi} + \tau B_2\right)\mathbf{e}_3. \tag{3.36}$$

For the usual MHD eigenmodes, namely the fast and slow magnetosonic modes and the Alfvén and entropy waves $\nabla\cdot\mathbf{B} = 0$, $\mathbf{e}_1 \cdot d\mathbf{B}/d\varphi = 0$ where $\mathbf{e}_1 = \mathbf{n}$, and (3.28) gives

$$\frac{dB_1}{d\varphi} = \kappa B_2. \tag{3.37}$$

Note that $B_n = \mathbf{B}\cdot\mathbf{n} \equiv B_1$ is in general not constant throughout the simple wave. The electric current in the wave is given by

$$\begin{aligned}\mathbf{J} &= \frac{1}{\mu_0}\nabla\times\mathbf{B} = \frac{1}{\mu_0}|\nabla\varphi|\mathbf{n}\times\frac{d\mathbf{B}}{d\varphi}\\ &= \frac{1}{\mu_0|F|}\left[-\left(\frac{dB_3}{d\varphi} + \tau B_2\right)\mathbf{e}_2 + \left(\frac{dB_2}{d\varphi} + \kappa B_1 - \tau B_3\right)\mathbf{e}_3\right].\end{aligned} \tag{3.38}$$

Note that the current diverges at points where $|F| = 1/|\nabla\varphi| = 0$, and that $\mathbf{J}$ is perpendicular to $\mathbf{n}$. The component of the current parallel to the magnetic field $\mathbf{J}\cdot\mathbf{e}_B$ is given by

$$\mathbf{J}\cdot\mathbf{e}_B = \frac{|\nabla\varphi|}{\mu_0 B}\left(B_3\frac{dB_2}{d\varphi} - B_2\frac{dB_3}{d\varphi} + \kappa B_1 B_3 - \tau\left(B_2^2 + B_3^2\right)\right). \tag{3.39}$$

Similarly the component of the fluid vorticity $\boldsymbol{\omega} = \nabla\times\mathbf{u}$ parallel to the magnetic field, $\boldsymbol{\omega}\cdot\mathbf{e}_B$, is given by

$$\boldsymbol{\omega}\cdot\mathbf{e}_B = \frac{|\nabla\varphi|}{B}\left(B_3\frac{du_2}{d\varphi} - B_2\frac{du_3}{d\varphi} + \kappa u_1 B_3 - \tau(u_3 B_3 + u_2 B_2)\right). \tag{3.40}$$

One of the distinguishing features of magnetoacoustic simple waves is that they have zero field aligned currents and vorticity, whereas Alfvén waves can have non-zero field aligned currents and vorticity.

## 4. The MHD eigensystem

The main ingredients in the construction of MHD simple waves are the eigenvalues and eigenvectors of the matrix $\mathbf{A} \equiv \mathbf{A}_n$ in (3.6). If we use the Serret–Frenet base, the matrix $\mathbf{A}$ corresponding to the primitive variables $\mathbf{W} = (\rho, \mathbf{u}^T, \mathbf{B}^T, p)^T$ in (3.2) and the conservative MHD system (2.1)–(2.4) with $\nabla\cdot\mathbf{B} \neq 0$ (note for our application to

https://doi.org/10.1017/S0022377809990596 Published online by Cambridge University Press

simple Alfvén waves $\nabla\cdot\mathbf{B}=0$), has the form

$$\mathbf{A}=\begin{pmatrix} u_1 & \rho & 0 & 0 & 0 & 0 & 0 & 0\\ 0 & u_1 & 0 & 0 & -\frac{B_1}{\mu\rho} & \frac{B_2}{\mu\rho} & \frac{B_3}{\mu\rho} & \frac{1}{\rho}\\ 0 & 0 & u_1 & 0 & -\frac{B_2}{\mu\rho} & -\frac{B_1}{\mu\rho} & 0 & 0\\ 0 & 0 & 0 & u_1 & -\frac{B_3}{\mu\rho} & 0 & -\frac{B_1}{\mu\rho} & 0\\ 0 & 0 & 0 & 0 & u_1 & 0 & 0 & 0\\ 0 & B_2 & -B_1 & 0 & 0 & u_1 & 0 & 0\\ 0 & B_3 & 0 & -B_1 & 0 & 0 & u_1 & 0\\ 0 & A & 0 & 0 & 0 & 0 & 0 & u_1 \end{pmatrix}. \tag{4.1}$$

The matrix (4.1) corresponds to the conservative MHD system used by Janhunen (2000) with $\nabla\cdot\mathbf{B}\neq 0$.

The right and left eigenvectors of the matrix $\mathbf{A}_n$ are defined by the eigenequations

$$(\mathbf{A}-\lambda\mathbf{I})\cdot\mathbf{R}=0,\quad \mathbf{L}\cdot(\mathbf{A}-\lambda\mathbf{I})=0,\quad \det(\mathbf{A}-\lambda\mathbf{I})=0, \tag{4.2}$$

where the eigenvalues $\{\lambda_j:\ 1\leqslant j\leqslant 8\}$ satisfy the eigenvalue equation $\det(\mathbf{A}-\lambda\mathbf{I})=0$. The left and right eigenvectors of the matrix $\mathbf{A}$, $\{\mathbf{L}_j\}$ and $\{\mathbf{R}_s\}$ $(j,s=1(1)8)$ in the general non-singular case can be chosen to satisfy the orthonormality conditions:

$$\mathbf{L}_j(\mathbf{n})\cdot\mathbf{R}_s(\mathbf{n})=\delta_{js}. \tag{4.3}$$

However, for the case of perpendicular propagation ($B_n=0$) there are multiple eigenvectors corresponding to $\lambda=\mathbf{u}_n$ (i.e., $\tilde{\mathbf{u}}_n=0$), and a separate analysis of the eigenvector equations is then necessary. In the case $B_n=0$ the diagonalized matrix system corresponds to a Jordan canonical matrix, in which the divergence wave mode solution corresponds to a Jordan mode (i.e., the matrix $\mathbf{A}$ is not diagonalizable in this case). Care is also required in normalizing the eigenvectors for parallel propagation at the so-called triple point for the case where the gas sound speed $a$ and the Alfvén speed $V_A$ have the same value (e.g., Brio and Wu 1988; Roe and Balsara 1996).

In the present paper, we are interested in the Alfvén eigenmodes. The backward and forward propagating Alfvén eigenmodes have eigenvalues

$$\lambda_A^{\pm}=u_n\pm V_{An},\quad \text{where}\quad u_n=\mathbf{u}\cdot\mathbf{n},\quad V_{An}=\mathbf{V}_A\cdot\mathbf{n}, \tag{4.4}$$

where $\mathbf{V}_A=\mathbf{B}/(\mu\rho)$ and $\mathbf{u}$ are the Alfvén velocity and flow velocity, respectively. The corresponding group velocities for the backward and forward eigenmodes from (3.12) are $\mathbf{V}_g^{\pm}=\mathbf{u}\pm\mathbf{V}_A$. The normalized right and left eigenvectors are

$$\mathbf{R}_A^{\pm}=\big(0,\mp(\mu\rho)^{-1/2}(\mathbf{n}\times\beta_\perp)^T,(\mathbf{n}\times\beta_\perp)^T,0\big)^T, \tag{4.5}$$

$$\mathbf{L}_A^{\pm}=\frac{1}{2}\big(0,\mp(\mu\rho)^{1/2}(\mathbf{n}\times\beta_\perp)^T,(\mathbf{n}\times\beta_\perp)^T,0\big), \tag{4.6}$$

where $\beta_\perp=\mathbf{B}_\perp/B_\perp$ and $\mathbf{B}_\perp=(\mathbf{I}-\mathbf{nn})\cdot\mathbf{B}$ is the component of $\mathbf{B}$ perpendicular to $\mathbf{n}$. The detailed form of the other eigenvalues, and left and right eigenvectors for the other eigenmodes of the matrix $\mathbf{A}$ are given in Appendix B.

https://doi.org/10.1017/S0022377809990596 Published online by Cambridge University Press

## 5. Alfvén simple waves

From (3.7) and the eigenvector equations (4.5), the eigenequations governing Alfvén simple waves are

$$\frac{d\rho}{d\varphi} = 0, \quad \frac{d\mathbf{u}}{d\varphi} = \mp\alpha(\varphi)\frac{\mathbf{n}\times\mathbf{B}}{\sqrt{\mu\rho}}, \quad \frac{d\mathbf{B}}{d\varphi} = \alpha(\varphi)\mathbf{n}\times\mathbf{B}, \quad \frac{dp}{d\varphi} = 0, \tag{5.1}$$

where $\alpha(\varphi)$ is an arbitrary function of $\varphi$. In (5.1) the $\mp$ signs correspond to the forward and backward Alfvén waves with eigenvalues $\lambda = u_n \pm V_{An}$, respectively. From (5.1),

$$\mathbf{n}\cdot\frac{d\mathbf{u}}{d\varphi} = 0, \quad \mathbf{n}\cdot\frac{d\mathbf{B}}{d\varphi} = 0, \quad \frac{d}{d\varphi}\left(\frac{B^2}{2}\right) = 0, \quad \frac{d}{d\varphi}(\mathbf{u}\pm\mathbf{V}_A) = 0. \tag{5.2}$$

Thus, the eigenequations have six integrals:

$$\mathbf{u}\pm\frac{\mathbf{B}}{\sqrt{\mu\rho}} = \mathbf{u}\pm\mathbf{V}_A = (V_1, V_2, V_3) = \mathbf{V} = const.,$$

$$p = c_4, \quad \rho = c_5, \quad B^2 = c_6. \tag{5.3}$$

The six integrals (5.3) imply the group velocity of the wave $\mathbf{V}$, the gas pressure $p$, the density $\rho$, and the magnetic pressure $p_B = B^2/(2\mu)$ are constant throughout the wave. The conditions that the gas pressure and density are constant throughout the wave implies that the entropy $S$ is also constant throughout the wave.

One further integral can, in principle, be obtained from the equation

$$\mathbf{n}\cdot\frac{d\mathbf{B}}{d\varphi} = 0, \tag{5.4}$$

which corresponds to Gauss' law $\nabla\cdot\mathbf{B} = 0$. In fact, (5.4) suggests two possible approaches to finding simple Alfvén wave solutions. In the first method, we specify the unit magnetic field vector $\mathbf{e}_B = \mathbf{B}/B$, and then determine $\mathbf{n}(\varphi)$ compatible with Gauss's equation (5.4) (note that $B$ is constant throughout the wave). A second approach is to specify the wave normal $\mathbf{n}(\varphi)$, and then obtain solutions of (5.4) for $\mathbf{B}(\varphi)$. The latter approach is in fact equivalent to solving the eigenequation

$$\frac{d\mathbf{B}}{d\varphi} = \alpha(\varphi)\mathbf{n}\times\mathbf{B}, \tag{5.5}$$

listed in (5.1). In Sec. 5.1, Alfvén wave solutions are obtained using the first approach (i.e., by specifying $\mathbf{e}_B(\varphi)$). In Sec. 5.2, the second approach is used in which $\mathbf{n}(\varphi)$ is given, from which solutions for $\mathbf{B}(\varphi)$ are obtained satisfying (5.5).

It is of interest to note from the integrals (5.3) that

$$\nabla\times\mathbf{B} = \mp\sqrt{\mu_0\rho}\,\nabla\times\mathbf{u}, \tag{5.6}$$

Hence the current is parallel, or anti-parallel, to the fluid vorticity according as the backward or forward Alfvén wave is being considered. In general Alfvén waves have field aligned currents and vorticity, but it is possible to construct Alfvén wave solutions with zero field aligned currents and vorticity. Equation (3.39) gives the field aligned current in the Serret–Frenet base (3.23).

### *5.1. Solutions with given* $\mathbf{e}_B(\varphi)$

In the following analysis we restrict our attention to the forward propagating Alfvén wave. Using the solution (3.9) with $f(\varphi) = \varphi/k_0$, where $k_0$ is a fixed normalizing

https://doi.org/10.1017/S0022377809990596 Published online by Cambridge University Press

wave number, gives

$$\varphi = k_0[\mathbf{r}\cdot\mathbf{n}(\varphi) - \lambda t] \tag{5.7}$$

for the wave phase. Since $\mathbf{n}(\varphi)$ is a unit vector and $B^2$ is constant in an Alfvén simple wave, then

$$\mathbf{n} = (\sin\Theta\cos\Phi, \sin\Theta\sin\Phi, \cos\Theta), \tag{5.8}$$

$$\mathbf{B} = B_0(\sin\alpha\cos\beta, \sin\alpha\sin\beta, \cos\alpha) \tag{5.9}$$

are representations of the wave normal $\mathbf{n}$ and magnetic field $\mathbf{B}$, where $\Theta$, $\Phi$, $\alpha$, and $\beta$ are functions of $\varphi$, and $B_0$ is a constant. Using the solution forms (5.8)–(5.9) for $\mathbf{n}$ and $\mathbf{B}$, Gauss' law (5.4) reduces to

$$\sin\Theta\cos\Phi\frac{d}{d\varphi}(\sin\alpha\cos\beta) + \sin\Theta\sin\Phi\frac{d}{d\varphi}(\sin\alpha\sin\beta) + \cos\Theta\frac{d}{d\varphi}\cos\alpha = 0, \tag{5.10}$$

in which $\alpha$, $\beta$, $\Theta$, and $\Phi$ are functions of $\varphi$.

From (3.12) the group velocity for the wave is

$$\mathbf{V}_g = \mathbf{u} + \mathbf{V}_A = (V_1, V_2, V_3), \tag{5.11}$$

whereas the normal phase speed of the wave:

$$\lambda = (\mathbf{u} + \mathbf{V}_A)\cdot\mathbf{n}. \tag{5.12}$$

The group velocity of the wave is a constant vector, but the phase speed $\lambda$ depends on $\mathbf{n}(\varphi)$. In general $d\lambda/d\varphi \neq 0$, unless $\mathbf{n}$ is a constant unit vector. Thus for general $\mathbf{n}(\varphi)$ the Alfvén wave is non-exceptional, and both centered and non-centered simple Alfvén waves can be constructed. This fact is not generally recognized, since the standard treatments of simple MHD waves assume that $\mathbf{n}$ is a constant unit vector.

Thus the analysis so far shows that the entropy $S$, density $\rho$, magnetic pressure $B^2/(8\pi)$, and $\mathbf{u} + \mathbf{V}_A$ remain constant throughout the forward Alfvén simple wave. Equation (5.10) implies there is a relationship between the angles $\Theta$ and $\Phi(\varphi)$ determining $\mathbf{n}$, and the magnetic field angles $\alpha(\varphi)$ and $\beta(\varphi)$. Note that Gauss' law $\mathbf{n}\cdot\mathbf{B}' = 0$, does not in general imply that $B_n$ is constant throughout the wave. For given functional forms $\alpha(\varphi)$, $\beta(\varphi)$, and $\Theta(\varphi)$, (5.10) for $\Theta \neq 0$ has solutions:

$$\Phi = \Phi_1 = -\epsilon - \sin^{-1}\left(\frac{R\cot\Theta}{A}\right), \quad \Phi = \Phi_2 = -\epsilon + \pi + \sin^{-1}\left(\frac{R\cot\Theta}{A}\right), \tag{5.13}$$

where

$$(P, Q, R) = \frac{1}{B_0}\frac{d\mathbf{B}}{d\varphi} = \frac{d}{d\varphi}(\sin\alpha\cos\beta, \sin\alpha\sin\beta, \cos\alpha),$$

$$\epsilon = \tan^{-1}\left(\frac{P}{Q}\right), \quad A = (P^2 + Q^2)^{1/2}. \tag{5.14}$$

Thus given $\alpha(\varphi)$, $\beta(\varphi)$ and $\Theta$, (5.13) determine the azimuthal angle $\Phi(\varphi)$ for $\mathbf{n}$. This leads to an infinite class of simple Alfvén wave solutions in which the geometry of the wave front depends on the solution for $\Phi(\varphi)$.

In the analysis below we give examples of simple Alfvén wave solutions.

https://doi.org/10.1017/S0022377809990596 Published online by Cambridge University Press

**Example 1.**

If $\Theta = 0$, (5.10) has the solution $\alpha = \alpha_0 = const.$, and no constraint is imposed on $\beta(\varphi)$. In this case we obtain the solution

$$\mathbf{n} = (0, 0, 1), \quad \varphi = k_0(z - \lambda t),$$

$$\mathbf{B} = B_0[\sin\alpha_0 \cos\beta(\varphi), \sin\alpha_0 \sin\beta(\varphi), \cos\alpha_0],$$

$$\mathbf{u} = -\frac{\mathbf{B}}{(\mu_0\rho)^{1/2}} + (V_1, V_2, V_3), \quad S = S_0, \quad \rho = \rho_0, \tag{5.15}$$

where $\rho_0$, $S_0$, and $k_0$ are constants. For $\beta = \varphi$, this is the usual planar simple Alfvén wave given in standard texts (e.g., Jeffrey and Taniuti 1964; Cabannes 1970).

The field lines for $\beta = \varphi$ obtained by integrating (3.18) have the form

$$\tilde{\mathbf{r}} = \frac{1}{k_0}(\tan\alpha_0 \sin\varphi, -\tan\alpha_0 \cos\varphi, \varphi), \quad \varphi = k_0(z - \lambda t), \tag{5.16}$$

where $\tilde{\mathbf{r}} = \mathbf{r} - \mathbf{V}t$ is the position in the group velocity frame. The curve (5.16) is a helix, with curvature $\kappa_B = \sin\alpha_0$, and torsion $\tau_B = \cos\alpha_0$ if one uses $\varphi$ as the parameter along the curve. From (3.38) the current $\mathbf{J}$ in the wave

$$\mathbf{J} = -\frac{1}{\mu_0} k_0 B_0 \sin\alpha_0(\cos\varphi, \sin\varphi, 0) \tag{5.17}$$

lies in the $xy$ plane and has a field aligned component:

$$\mathbf{J}\cdot\mathbf{e}_B = -\frac{1}{\mu_0} k_0 B_0 \sin^2\alpha_0. \tag{5.18}$$

The helical field configuration (5.16) is illustrated in Fig. 1.

**Example 2**

An example of a non-planar Alfvén wave is obtained by choosing $\alpha = \alpha_0 = const.$, $\beta = \varphi$, and $\Theta = \Theta_0$. In this case (5.13) yield the solution $\Phi = \varphi$. The resultant Alfvén wave solution is described by the equations:

$$\mathbf{n} = [\sin\Theta_0 \cos\varphi, \sin\Theta_0 \sin\varphi, \cos\Theta_0],$$

$$f(\varphi) = [\sin\Theta_0(x\cos\varphi + y\sin\varphi) + z\cos\Theta_0 - \lambda t],$$

$$\mathbf{B} = B_0(\sin\alpha_0 \cos\varphi, \sin\alpha_0 \sin\varphi, \cos\alpha_0),$$

$$\mathbf{u} = -\frac{\mathbf{B}}{(\mu_0\rho)^{1/2}} + (V_1, V_2, V_3), \quad \rho = \rho_0, \quad S = S_0, \quad f(\varphi) = \frac{\varphi}{k_0}. \tag{5.19}$$

Centered simple Alfvén waves with $f(\varphi) = 0$ are obtained by letting $k_0 \to \infty$ in the solution (5.19). In contrast to Example 1, the wave phase is given in implicit form. The equation for $\varphi$ can also be written in the form

$$\varphi = k_0[r\sin\Theta_0 \cos(\varphi - \theta) + z\cos\Theta_0 - \lambda t], \tag{5.20}$$

where $x = r\cos\theta$ and $y = r\sin\theta$.

The field line differential equations (3.30) may be integrated to yield the field lines for the wave in the form (see Appendix C):

$$\tilde{x} = -[\tilde{q}_2 \sin\varphi + \cos\varphi(\tilde{q}_3 \cos\Theta_0 - \tilde{q}_1 \sin\Theta_0)],$$

$$\tilde{y} = \tilde{q}_2 \cos\varphi + \sin\varphi(\tilde{q}_1 \sin\Theta_0 - \tilde{q}_3 \cos\Theta_0),$$

$$\tilde{z} = \cos\Theta_0 \tilde{q}_1 + \sin\Theta_0 \tilde{q}_3, \tag{5.21}$$

https://doi.org/10.1017/S0022377809990596 Published online by Cambridge University Press

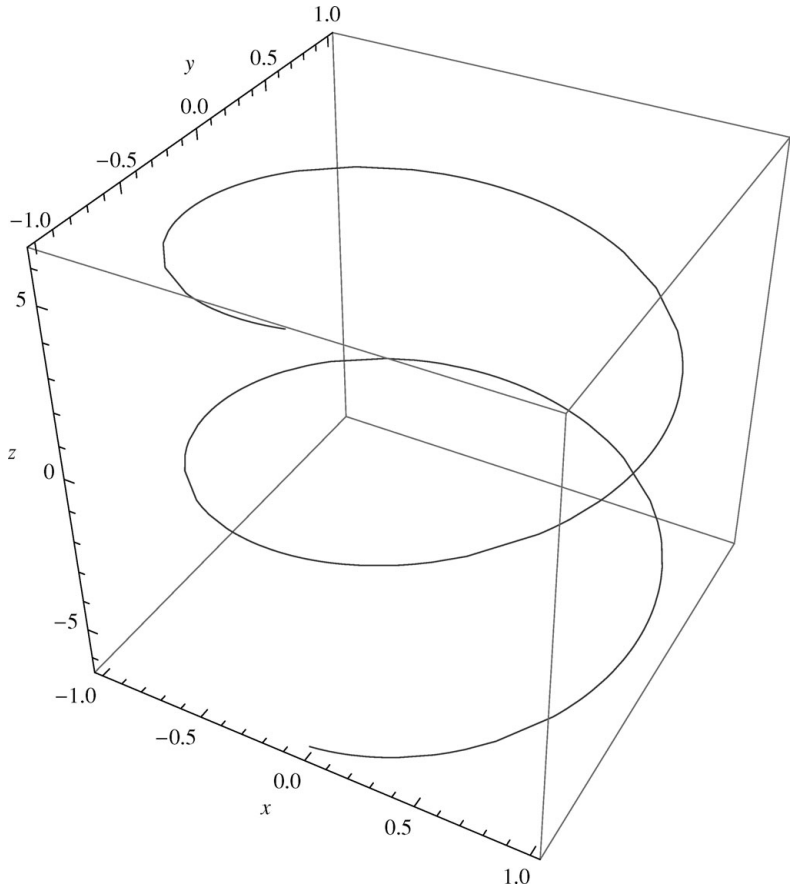


**Figure 1.** Magnetic field line for the 1D, planar simple Alfvén wave (5.15), with $\alpha_0 = \pi/4$, $k_0 = 1$. The wave is a traveling, non-centered simple wave, propagating along the $z$-axis. The wave normal $\mathbf{n} = (0, 0, 1)$. The current is finite and azimuthal about the $z$-axis.

where

$$\tilde{q}_1 = \frac{\varphi}{k_0}, \quad \tilde{q}_2 = r_0 \sin(\zeta - \zeta_0) - \frac{\tan\alpha_0}{k_0 \cos\Theta_0}, \quad \tilde{q}_3 = \frac{r_0 c_0}{\cos\Theta_0}\cos(\zeta - \zeta_0) + \frac{\varphi \tan\Theta_0}{k_0},$$

$$\zeta = c_0\varphi, \quad c_0 = \left(\frac{\cos\Theta_0 \cos\alpha_0}{\cos(\Theta_0 - \alpha_0)}\right)^{1/2}, \tag{5.22}$$

$r_0$ is an arbitrary constant, and $\tilde{q}_1$, $\tilde{q}_2$, and $\tilde{q}_3$ ((3.26) specify the position $\tilde{\mathbf{r}}$ in the group velocity frame). In order to gain insight into the geometry of the field lines (5.21) it is instructive to consider the cases of centered ($k_0 \to \infty$) and non-centered simple Alfvén waves separately.

### 5.2. *Centered simple waves*

The simplest example of a centered simple Alfvén wave is obtained by letting $k_0 \to \infty$ and setting $\alpha_0 = \pi/2$ and $\Theta_0 = \pi/2$ in the solutions (5.19). This example has been discussed by Barnes (1976). The solutions (5.19) for $\mathbf{n}$ and $\mathbf{B}$ reduce to

$$\mathbf{n} = (\cos\varphi, \sin\varphi, 0), \quad \mathbf{B} = B_0(\cos\varphi, \sin\varphi, 0). \tag{5.23}$$

https://doi.org/10.1017/S0022377809990596 Published online by Cambridge University Press

For the centered simple Alfvén wave, the equation of the wave front is

$$\tilde{x}\cos\varphi + \tilde{y}\sin\varphi = 0, \quad \text{or} \quad \varphi = \pi - \tan^{-1}\left(\frac{\tilde{x}}{\tilde{y}}\right),$$

$$\tilde{x} = \tilde{r}\cos\tilde{\theta}, \quad \tilde{y} = \tilde{r}\sin\tilde{\theta}, \quad \tilde{r}^2 = \tilde{x}^2 + \tilde{y}^2. \tag{5.24}$$

Either using (3.18) or (3.30) we obtain

$$(\tilde{x}, \tilde{y}, \tilde{z}) = (r_0\sin\varphi, -r_0\cos\varphi, \tilde{z}_0), \tag{5.25}$$

for the field lines. Hence the field lines consist of concentric circles $(\tilde{x}(\varphi), \tilde{y}(\varphi), \tilde{z}_0)$ of radius $r_0$ in each plane $\tilde{z} = \tilde{z}_0 = const.$

Wave breaking for the simple wave occurs on the wave envelope of the family of phase fronts $G = f(\varphi) - \tilde{\mathbf{r}}\cdot\mathbf{n}(\varphi) = 0$. In the present example, $f(\varphi) = 0$ and $G(\varphi) = -\tilde{\mathbf{r}}\cdot\mathbf{n}$. On the envelope $(\tilde{x}, \tilde{y})$ satisfies simultaneously the equations $G = 0$ and $G_\varphi \equiv F = 0$, i.e.,

$$G = -(\tilde{x}\cos\varphi + \tilde{y}\sin\varphi) = 0, \quad G_\varphi = \tilde{x}\sin\varphi - \tilde{y}\cos\varphi = 0. \tag{5.26}$$

Equations (5.26) can be written in the matrix form $\mathbf{A}\tilde{\mathbf{x}} = 0$ where $\tilde{\mathbf{x}} = (\tilde{x}, \tilde{y})$. Because $\det\mathbf{A} = 1$, (5.26) only have the trivial solution $(\tilde{x}, \tilde{y}) = (0, 0)$. Thus the wave breaks on the $\tilde{z}$-axis. An alternative way to view wave breaking is to evaluate the current $\mathbf{J}$ in the wave, namely

$$\mathbf{J} = \frac{B_0 k}{\mu_0}\mathbf{e}_z = \frac{B_0}{\mu_0(\tilde{x}\sin\varphi - \tilde{y}\cos\varphi)}. \tag{5.27}$$

On the field line (5.25) with $\tilde{r} = r_0$, the current (5.27) has the form

$$\mathbf{J} = \frac{B_0}{\mu_0\tilde{r}}\mathbf{e}_z. \tag{5.28}$$

Thus, the current blows up on the wave envelope where $\tilde{r} = 0$.

The magnetic field and current configuration are illustrated in Fig. 2. The magnetic field is generated by the current (5.27) which is singular on the $\tilde{z}$-axis. The wave normal $\mathbf{n}$ and the magnetic field $\mathbf{B}$ are parallel, and directed in the azimuthal direction in the $\tilde{x}\tilde{y}$ plane. Note that $\varphi = \pi/2 + \tilde{\theta}$, where $\tilde{x} = r_0\cos\tilde{\theta}$, $\tilde{y} = r_0\sin\tilde{\theta}$ gives the position of a point on the field line at radius $\tilde{r} = r_0$ from the $\tilde{z}$-axis. The magnetic field (5.23) corresponds to the magnetic potential $\mathbf{A} = -B_0\tilde{r}\mathbf{e}_z$ (i.e., $\mathbf{B} = \nabla\times\mathbf{A}$).

*Centered wave with $\alpha_0 \neq \pi/2$ and $\Theta_0 = \pi/2$*

The simplest generalization of the Barnes solution is obtained by setting $\alpha_0 \neq \pi/2$ and $\Theta_0 = \pi/2$ in the solution (5.19). For a centered wave $f(\varphi) = 0$ in (5.19). For this solution,

$$\mathbf{n} = (\cos\varphi, \sin\varphi, 0), \quad \mathbf{B} = B_0(\sin\alpha_0\cos\varphi, \sin\alpha_0\sin\varphi, \cos\alpha_0), \tag{5.29}$$

The field line equations (3.18) for the solution (5.29) integrate to give the helix

$$\tilde{\mathbf{r}} = -r_0\,(\sin\varphi, -\cos\varphi, \cot\alpha_0\ \varphi)\,. \tag{5.30}$$

By noting that $\varphi = \pi/2 + \theta$ where $(r, \theta, z)$ are cylindrical polar coordinates, the magnetic field (5.29) can be written in the form

$$\mathbf{B} = B_0\sin\alpha_0\mathbf{e}_\theta + B_0\cos\alpha_0\mathbf{e}_z. \tag{5.31}$$

https://doi.org/10.1017/S0022377809990596 Published online by Cambridge University Press

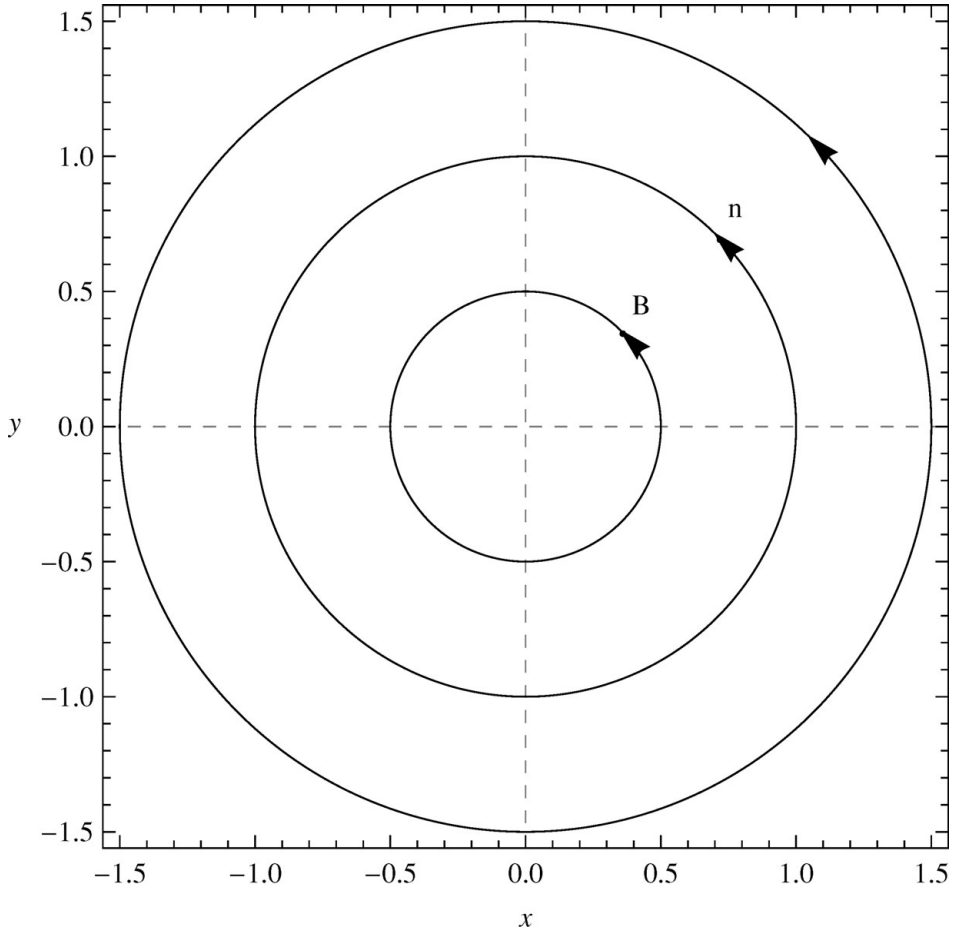


**Figure 2.** The magnetic field lines and wave normal for the Barnes (1976) simple Alfvén wave solution. The wave normal **n** and magnetic induction **B** are parallel and are directed in the azimuthal direction ($\mathbf{n} = (\cos\varphi, \sin\varphi, 0)$ where $\varphi$ is the wave phase). The wave phase fronts are planes $\varphi = const.$ perpendicular to **B**, passing through the origin of the $xy$ plane. The current is spatially non-uniform, directed along the $\tilde{z}$-axis, and diverges as $\tilde{r} \to 0$, where $\tilde{r} = (\tilde{x}^2 + \tilde{y}^2)^{1/2}$ is radial distance from the $\tilde{z}$-axis.

Thus, **B** has a constant azimuthal component $B_\theta = B_0 \sin\alpha_0$, a constant $z$ component $B_z = B_0 \cos\alpha_0$ and $B_r = 0$ in cylindrical polar coordinates. The field lines (5.30) are the same as the non-centered, one-dimensional (1D), planar, traveling Alfvén wave solution in (5.15)–(5.16) (setting $r_0 = -\tan\alpha_0/k_0$ in (5.30) gives the field lines (5.16)). However, the two solutions are clearly physically different. Solution (5.15)–(5.16) has wave normal $\mathbf{n} = (0, 0, 1)$ directed along the $z$-axis, and has a non-singular azimuthal circular current $\mathbf{J} \parallel (\cos\varphi, \sin\varphi, 0)$, which is finite in all space. The modified Barnes solution (5.30) has an azimuthal wave normal $\mathbf{n} = (\cos\varphi, \sin\varphi, 0)$, and the current $\mathbf{J} = B_0 \sin\alpha_0/(\mu_0\tilde{r})(0, 0, 1)$ is directed along the $\tilde{z}$-axis, and diverges as $\tilde{r} \to 0$ on the $\tilde{z}$-axis. The field lines for the simple wave (5.29)–(5.30) have a helical spiral structure as illustrated in Fig. 1.

https://doi.org/10.1017/S0022377809990596 Published online by Cambridge University Press

The above example illustrates that two distinct Alfvén wave solutions can have the same field line structure, but have distinct wave speeds, wave normals, and currents.

*Centered waves with $\alpha_0 \neq \pi/2$ and $\Theta_0 \neq \pi/2$*

A more complex model of a centered simple Alfvén wave is obtained by letting $k_0 \to \infty$ in the solution (5.19), but choosing $\alpha_0 \neq \pi/2$ and $\Theta_0 \neq \pi/2$ (i.e., $f(\varphi) = 0$). The equation for the wave phase $\varphi$ in (5.19) reduces to

$$\tilde{x}\cos\varphi + \tilde{y}\sin\varphi + \tilde{z}\cot\Theta_0 = 0. \tag{5.32}$$

Equation (5.32) has solutions $\varphi = \varphi_1$ and $\varphi = \varphi_2$ given by

$$\varphi_1 = -\tan^{-1}\left(\frac{\tilde{x}}{\tilde{y}}\right) - \sin^{-1}\left(\frac{\tilde{z}\cot\Theta_0}{\tilde{r}}\right),$$

$$\varphi_2 = \pi + \sin^{-1}\left(\frac{\tilde{z}\cot\Theta_0}{\tilde{r}}\right) - \tan^{-1}\left(\frac{\tilde{x}}{\tilde{y}}\right). \tag{5.33}$$

It turns out that the solution $\varphi = \varphi_2$ is the relevant solution for $\varphi$, for which $F = G_\varphi = -\tilde{r}\cdot\mathbf{n}'(\varphi) > 0$. The function $F \equiv 1/|\nabla\varphi|$ from (3.11), (3.29), and (5.33) (using $\varphi = \varphi_2$) is given by

$$F = -\kappa\tilde{q}_2 = \sin\Theta_0(\tilde{r}^2 - \tilde{z}^2\cot^2\Theta_0)^{1/2}. \tag{5.34}$$

From (5.34) we require

$$|\tilde{z}| < \tilde{r}\tan\Theta_0 \tag{5.35}$$

for a real solution. The gradient $|\nabla\varphi| \to \infty$ on the cone $\tilde{z} = \tilde{r}\tan\Theta_0$. The current $\mathbf{J}$ is given by

$$\mathbf{J} = \frac{B_0\sin\alpha_0}{\mu_0(\tilde{r}^2 - \tilde{z}^2\cot^2\Theta_0)^{1/2}}(-\cot\Theta_0\cos\varphi, -\cot\Theta_0\sin\varphi, 1),$$

$$\equiv \frac{B_0\sin\alpha_0}{\mu_0|\tilde{q}_2|\sin\Theta_0}\mathbf{e}_3, \tag{5.36}$$

Since $\tilde{q}_1 \equiv 0$ for a centered wave, the field line solutions (5.21) simplify to

$$\tilde{x} = -(\tilde{q}_2\sin\varphi + \tilde{q}_3\cos\Theta_0\cos\varphi), \quad \tilde{y} = \tilde{q}_2\cos\varphi - \tilde{q}_3\cos\Theta_0\sin\varphi, \quad \tilde{z} = \tilde{q}_3\sin\Theta_0, \tag{5.37}$$

where

$$\tilde{q}_2 = r_0\sin(\zeta - \zeta_0), \quad \tilde{q}_3 = \frac{r_0 c_0}{\cos\Theta_0}\cos(\zeta - \zeta_0), \quad \zeta = c_0\varphi. \tag{5.38}$$

It is of interest to note that in $(\tilde{q}_2, \tilde{q}_3)$ space, the field line is an ellipse:

$$\tilde{q}_2^2 + \left(\frac{\cos\Theta_0\tilde{q}_3}{c_0}\right)^2 = r_0^2. \tag{5.39}$$

From (5.38) the singular cone $F = 0$ corresponds to points along the field line

$$c_0(\varphi - \varphi_0) = n\pi, \tag{5.40}$$

where $c_0$ is defined in (5.22), and $n$ is an integer. Equation (5.40) gives the value of $\varphi$ on the field line where it intersects the singular cone. In effect the current singularity

https://doi.org/10.1017/S0022377809990596 Published online by Cambridge University Press

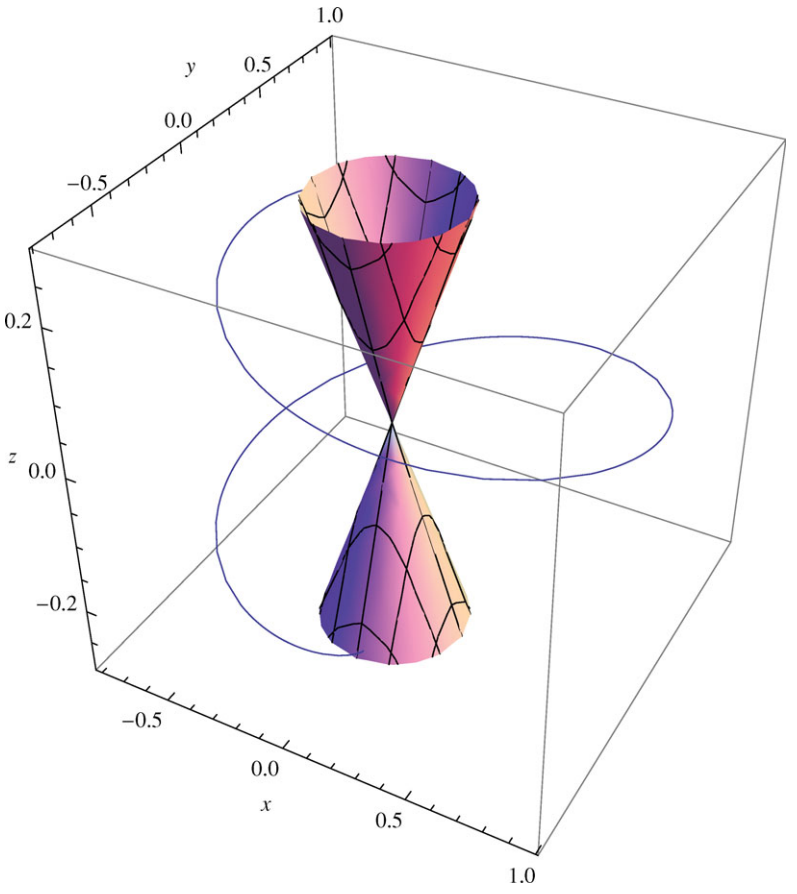


**Figure 3.** (Color online) Sample magnetic field line for centered simple Alfvén wave, which generalizes the Barnes simple wave (Barnes 1976). The current is singular on the cone $\tilde{z} = \tilde{r}\tan\Theta_0$, where $\tilde{r} = (\tilde{x}^2 + \tilde{y}^2)^{1/2}$ is radial distance from the $\tilde{z}$-axes. $\Theta_0 = 45^\circ$ and $\alpha_0 = 85^\circ$. $\varphi = 0$ at the top of the figure, and $\varphi = \pi/c_0$ at the bottom of the figure, where the field line intersects the cone. The Barnes solution is recovered by setting $\alpha_0 = 90^\circ$ and $\Theta_0 = 90^\circ$

present along the $\tilde{z}$-axis in the example of Fig. 2 is now spread out over the cone $\tilde{z} = \tilde{r}\tan\Theta_0$.

Figure 3 shows an example of a field line solution for the centered simple wave described in (5.32) et seq. with $\varphi_0 = 0$, $\alpha_0 = 85^\circ$, $\Theta_0 = 45^\circ$, and $r_0 = 1$. The field line starts at the top of the figure, where $\varphi = 0$ and ends up at the bottom of the figure at $\varphi = \pi/c_0$. The field line has a spiral type structure and both begins and ends on the current sheet $\tilde{z} = \tilde{r}\tan\Theta_0$.

Figure 4 shows the same field line and current sheet (the cone) as in Fig. 3, but extended from $\varphi = 0$ to $\varphi = 2\pi/c_0$. Figure 5 shows the field line in Fig. 4, without the current sheet. Notice the kink or cusp in the magnetic field line at the bottom of the figure where $\varphi = \pi/c_0$. It was noted in (3.32) et seq. that the tangent vector to the field line $d\mathbf{x}/d\varphi = F\mathbf{B}/B_1 = (0,0,0)$ on the wave envelope (i.e., on the current sheet where $F = 0$). This is the point where the cusp is located. In the present example $F = -r_0\sin\Theta_0\sin(c_0\varphi)$ and $F = 0$ when $\varphi = n\pi/c_0$. Thus, there

https://doi.org/10.1017/S0022377809990596 Published online by Cambridge University Press

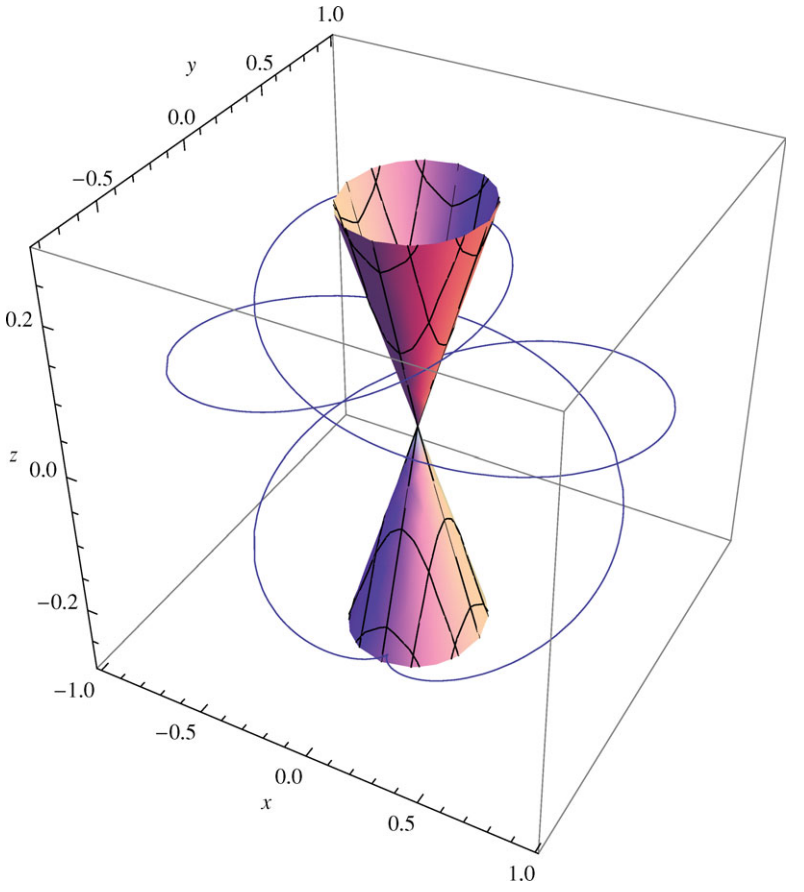


**Figure 4.** (Color online) Field lines and current sheet for the centered wave of Fig. 3, for $0 \leqslant \varphi \leqslant 2\pi/c_0$.

are cusps in the field line at the points, where $\varphi = n\pi/c_0$ ($n$ integer), for the present example.

Consider the current for the simple waves illustrated in Figs. 3–5. The current in the simple wave (5.36) can be written in the form

$$\mathbf{J} = \frac{B_0 \sin\alpha_0}{\mu_0 \sin\Theta_0} \frac{\mathbf{e}_3}{[\tilde{r}^2 - \tilde{z}^2 \cot\Theta_0]^{1/2}}, \tag{5.41}$$

where

$$\begin{aligned} \mathbf{e}_3 &= -\cos\Theta_0 \cos(\varphi - \theta)\mathbf{e}_r - \cos\Theta_0 \sin(\varphi - \theta)\mathbf{e}_\theta + \sin\Theta_0 \mathbf{e}_z, \\ &= \frac{\tilde{z}\cos^2\Theta_0}{\tilde{r}\sin\Theta_0}\mathbf{e}_r - \sigma_s \cos\Theta_0 \left(1 - \frac{\tilde{z}^2 \cot^2\Theta_0}{\tilde{r}^2}\right)^{1/2} \mathbf{e}_\theta + \sin\Theta_0 \mathbf{e}_z, \end{aligned} \tag{5.42}$$

where $\sigma_s = \mathrm{sgn}(\sin(\varphi - \theta))$ and $\mathbf{e}_r$, $\mathbf{e}_\theta$, and $\mathbf{e}_z$ are unit vectors using cylindrical coordinates with the polar axis along the $z$ direction. On the current sheet $\tilde{z} = \pm\tilde{r}\tan\Theta_0$, $\mathbf{J} \to \infty$ and

$$\mathbf{e}_3 = \pm\cos\Theta_0 \mathbf{e}_r + \sin\Theta_0 \mathbf{e}_z. \tag{5.43}$$

https://doi.org/10.1017/S0022377809990596 Published online by Cambridge University Press

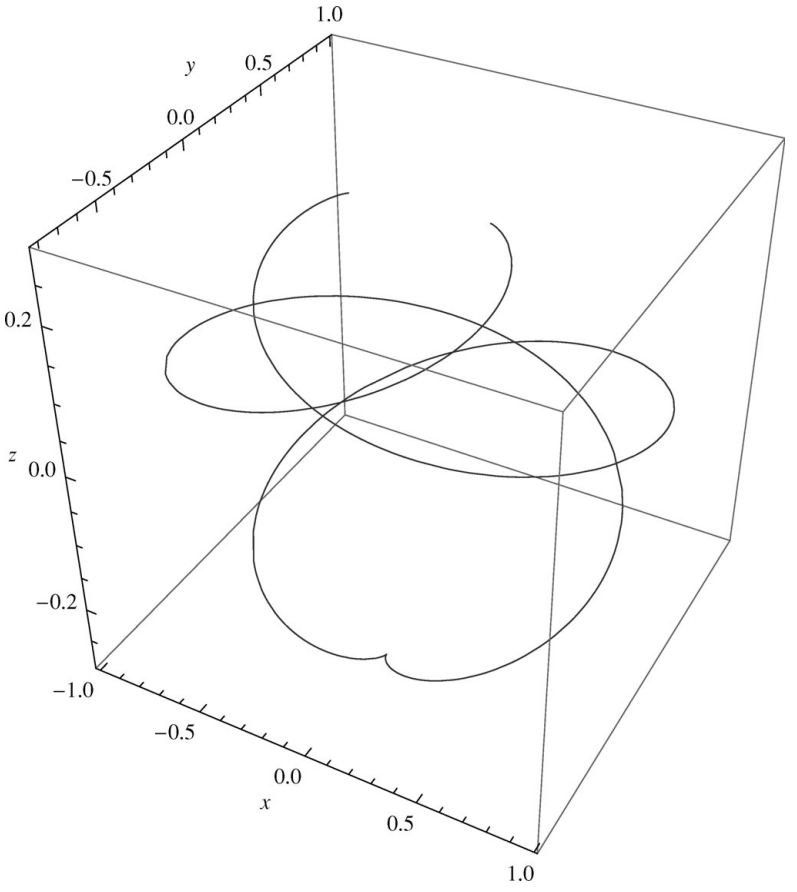


**Figure 5.** Field lines for the centered wave of Fig. 4 for $0 \leqslant \varphi \leqslant 2\pi/c_0$. Note the cusp in the field line at $\varphi = \pi/c_0$ at the bottom of the figure. In general, cusps occur at $\varphi = n\pi/c_0$ ($n$ integer) when the field line hits the current sheet (the cone) in Fig. 4.

Thus, the current streamlines on the sheet consists of the straight line generators of the cone. Note there is no azimuthal component to the current on the sheet.

At large radii $\tilde{r} \gg |\tilde{z}| \cot \Theta_0$, the current is approximately given by

$$\mathbf{J} \sim \frac{B_0 \sin \alpha_0}{\mu_0 \sin \Theta_0 \tilde{r}} \left(-\sigma_s \cos \Theta_0 \mathbf{e}_\theta + \sin \Theta_0 \mathbf{e}_z\right). \tag{5.44}$$

Thus, at large radii, the current has a helical structure, with no radial component, whereas at small radii, the current has no azimuthal component.

An alternative analysis of the current streamlines is to use the field line streamlines (3.30) but with $(B_1, B_2, B_3)$ replaced by $(J_1, J_2, J_3)$. In the present application, $J_1 = J_2 = 0$ and $J_3 \neq 0$ and $(\kappa_1, \kappa_2, \kappa_3) \equiv (\tau, 0, \kappa)$ where $\tau = \cos \Theta_0$ and $\kappa = \sin \Theta_0$. The current streamline equations take the form

$$\frac{d\varphi}{d\lambda} = 0, \quad \frac{d\tilde{q}_2}{d\lambda} = 0, \quad \frac{d\tilde{q}_3}{d\lambda} = FJ_3 = \frac{B_0 \sin \alpha_0}{\mu_0}, \tag{5.45}$$

https://doi.org/10.1017/S0022377809990596 Published online by Cambridge University Press

where $\lambda$ is the parameter along the streamlines. Equations (5.45) have first integrals $\tilde{q}_2 = \tilde{q}_{2c} = const.$ and $\varphi = \varphi_c = const.$. The latter two integrals, in turn, imply

$$\tilde{x}\cos\varphi_c + \tilde{y}\sin\varphi_c + \tilde{z}\cot\Theta_0 = 0,$$

$$-\tilde{x}\sin\varphi_c + \tilde{y}\cos\varphi_c = \tilde{q}_{2c}. \tag{5.46}$$

The streamlines for **J** follow by eliminating $\varphi_c$ between the two equations in (5.46). In particular, for the case $\tilde{q}_{2c} = 0$, (5.46) give the envelope of the family of wave fronts in the form

$$\tilde{z} = -\sigma_c \tan\Theta_0 \tilde{r}, \quad \sec\varphi_c = \frac{\sigma_c \tilde{r}}{\tilde{x}}, \quad \sigma_c = \pm 1. \tag{5.47}$$

Thus the current streamlines are the straight line generators of the cone. Clearly, (5.46) may also be used to determine the current streamlines at large radii $\tilde{r} \gg |\tilde{z}|\cot\Theta_0$, by eliminating $\varphi_c$ in (5.46) for $\tilde{q}_{2c} \gg 1$.

### *5.3. Non-centered simple waves*

A non-centered simple wave is obtained from the solution (5.19) by choosing $f(\varphi) = \varphi/k_0$ where $k_0$ is finite. The centered simple waves in Figs. 3–4 occur for $k_0 \to \infty$.

The field lines for the solution (5.19) are given by (5.21)–(5.22). The wave front equation $G(\varphi) = f(\varphi) - \tilde{\mathbf{r}}\cdot\mathbf{n}(\varphi)$, is given by

$$G = \frac{\varphi}{k_0} - \sin\Theta_0(\tilde{x}\cos\varphi + \tilde{y}\sin\varphi) - \cos\Theta_0\tilde{z} = 0, \tag{5.48}$$

Using the field line solutions (5.21)–(5.22) for $(\tilde{x}, \tilde{y}, \tilde{z})$ it is straightforward to verify $G = 0$ on the field lines (as it should). The function

$$F = G_\varphi = \frac{1}{k_0} - \sin\Theta_0\,(\tilde{y}\cos\varphi - \tilde{x}\sin\varphi) \tag{5.49}$$

determines when the wave breaks (i.e., $|\nabla\varphi| \to \infty$ as $F \to 0$). On the field lines (5.21)–(5.22),

$$F = \frac{1}{k_0} - \sin\Theta_0\tilde{q}_2 \equiv \frac{1 + \tan\alpha_0\tan\Theta_0}{k_0} - r_0\sin\Theta_0\sin[c_0(\varphi - \varphi_0)]. \tag{5.50}$$

From (5.50), $F = 0$ if $\varphi$ satisfies the equation:

$$\sin[c_0(\varphi - \varphi_0)] = \frac{1 + \tan\alpha_0\tan\Theta_0}{k_0 r_0 \sin\Theta_0}. \tag{5.51}$$

The condition (5.51) to have solutions for $\varphi$ is the right-hand side of (5.51) has magnitude less than unity. If this is the case, then the wave breaks at values of $\varphi$ satisfying the equation

$$\varphi = \varphi_0 + \varphi_c + n\pi \quad (n \text{ integer}) \quad \text{where} \quad \varphi_c = \sin^{-1}\left(\frac{1 + \tan\alpha_0\tan\Theta_0}{k_0 r_0 \sin\Theta_0}\right). \tag{5.52}$$

Assuming $0 < \Theta_0 \leqslant \pi/2$ and $0 < \alpha_0 \leqslant \pi/2$, the condition for the wave not to break (i.e., to be free of current sheets) is

$$k_0 r_0 < \frac{1 + \tan\alpha_0\tan\Theta_0}{\sin\Theta_0}. \tag{5.53}$$

The radius $r_0$ characterizes in some sense, the location of the field line from the $z$-axis. Clearly for large enough $r_0$, (5.53) will be violated, and the wave will break.

https://doi.org/10.1017/S0022377809990596 Published online by Cambridge University Press

It is also obvious from (5.53) that waves with smaller $k_0$ will be more stable (i.e., will be less prone to break).

The envelope of the family of phase fronts (5.48) is obtained from the simultaneous solution of (5.48) and (5.49). This surface from (5.48)–(5.49) can be expressed in the parametric form:

$$\tilde{x}(\varphi,\tilde{z}) = -\tilde{z}\cot\Theta_0\cos\varphi + \frac{\varphi\cos\varphi - \sin\varphi}{k_0\sin\Theta_0},$$

$$\tilde{y}(\varphi,\tilde{z}) = -\tilde{z}\cot\Theta_0\sin\varphi + \frac{\varphi\sin\varphi + \cos\varphi}{k_0\sin\Theta_0}. \tag{5.54}$$

Equations (5.54) reduce to the cone $\tilde{r}^2 = \tilde{z}^2\cot^2\Theta_0^2$ in the limit as $k_0 \to \infty$ where $\tilde{r} = (\tilde{x}^2 + \tilde{y}^2)^{1/2}$ is cylindrical radius from the $\tilde{x}$-axis. For finite $k_0 \neq 0$, (5.49)–(5.50) can be written in the form

$$\tilde{r}\cos(\varphi+\epsilon) = \frac{1}{k_0\sin\Theta_0}, \quad \tilde{r}\sin(\varphi+\epsilon) = \frac{\varphi}{k_0\sin\Theta_0} - \tilde{z}\cot\Theta_0, \tag{5.55}$$

where

$$\epsilon = \tan^{-1}\left(\frac{\tilde{x}}{\tilde{y}}\right), \quad \tilde{r} = (\tilde{x}^2+\tilde{y}^2)^{1/2}. \tag{5.56}$$

By squaring and adding (5.55) we obtain

$$\tilde{r}^2 = \frac{1}{k_0^2\sin^2\Theta_0} + \left(\frac{\varphi}{k_0\sin\Theta_0} - \tilde{z}\cot\Theta_0\right)^2. \tag{5.57}$$

From (5.57) it follows that the envelope is located at $\tilde{r} > (k_0\sin\Theta_0)^{-1}$. From (5.57) and (5.55) we obtain two independent equations for $\varphi$, namely

$$\varphi = k_0\tilde{z}\cos\Theta_0 - \sigma_z\left[k_0^2\tilde{r}^2\sin^2\Theta_0 - 1\right]^{1/2}, \quad \varphi+\epsilon = \sigma_c\arccos\left(\frac{1}{k_0\tilde{r}\sin\Theta_0}\right), \tag{5.58}$$

where $\sigma_z = \pm 1$ and $\sigma_c = \mp 1$ (it turns out that $\sigma_z = -\sigma_c$ in order for these formulae to be consistent with (5.54)). Eliminating $\varphi$ between the two equations in (5.58) gives the wave envelope in cylindrical polar coordinates in the form

$$\tilde{x} = \tilde{r}\cos\theta, \quad \tilde{y} = \tilde{r}\sin\theta,$$

$$\tilde{z} = \frac{1}{k_0\cos\Theta_0}\left[\theta - \frac{1}{2}\pi + \sigma_c\arccos\left(\frac{1}{k_0\tilde{r}\sin\Theta_0}\right) + \sigma_z\sqrt{(k_0\tilde{r}\sin\Theta_0)^2 - 1}\right]. \tag{5.59}$$

Here $\theta = \pi/2 - \epsilon$ relates $\epsilon$ to the cylindrical polar azimuthal coordinate $\theta$ and $\sigma_c = -\sigma_z$. The $\sigma_z = \pm 1$ branches of the surface correspond to the upper and lower $\tilde{z}$ branches of the surface. Note that the surface is located in the region $\tilde{r} > 1/(k_0\sin\Theta_0)$.

Figure 6 shows the current sheet and field lines for the non-centered simple Alfvén wave for $k_0 = 200$, $r_0 = 1$, $\theta_0 = 45^\circ$ and $\alpha_0 = 85^\circ$. The field lines are shown for $0 < \varphi < 3\pi/c_0$. The current sheet (5.54) is shown for $0 < \varphi < 2\pi$ (the current sheet looks more complicated if shown for a larger range of $z$ and $\varphi$). The field line intersects the wave envelope at $\varphi = (\varphi_c + n\pi)/c_0$ ($n$ integer), where $\varphi_c = 5.0424^\circ$ (see (5.52)). The field line, without the current sheet is shown in Fig. 7. There are cusps when the field line intersects the current sheet.

https://doi.org/10.1017/S0022377809990596 Published online by Cambridge University Press

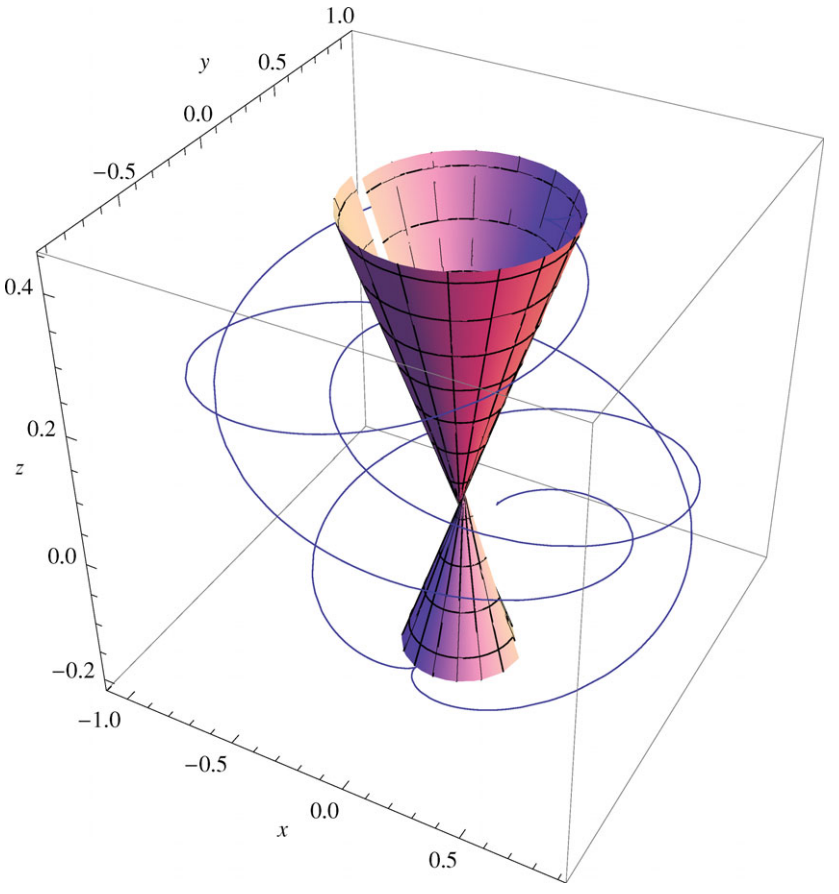


**Figure 6.** (Color online) Field lines and singular current surface for the non-centered simple Alfvén wave (5.19) for $k_0 = 200$, $r_0 = 1$, and $0 < \varphi < 3\pi/c_0$. Note the distortion of the current sheet from a conical surface due to finite $k_0$. The field line has cusps at $\varphi = (\varphi_c + n\pi)/c_0$, where $\varphi_c = 5.0424°$ (see (5.52)).

Figure 8 shows a field line and the current sheet for $k_0 = 10$ and $r_0 = 1$, and the same value of the parameters as in Fig. 6. In this case there are no real solutions of (5.51) for $\varphi$ for which $F = 0$. Thus, the field lines do not intersect the current sheet in this case. The current sheet was determined by using the polar coordinate representation (5.59). Figure 9 shows the field line. There are no kinks in the field line and no points at which the field line intersects the current sheet surface (5.54).

**Example 3**

As a third example, the choice $\alpha = \varphi$, $\beta = \varphi$ and $\Theta = \Theta_0$ in (5.13) yields the solution

$$\alpha = \varphi, \quad \beta = \varphi, \quad \Phi = 2\varphi - \frac{\pi}{2} + \sin^{-1}(\sin\varphi \cot\Theta_0), \tag{5.60}$$

for $\alpha$, $\beta$, and $\Phi$. Simpler solutions are obtained for special values of $\Theta_0$. In particular, if $\Theta_0 = 1/2\pi$ yields the solution

$$\alpha = \varphi, \quad \beta = \varphi, \quad \Phi = 2\varphi - \frac{\pi}{2}, \quad \Theta_0 = \frac{\pi}{2}. \tag{5.61}$$

https://doi.org/10.1017/S0022377809990596 Published online by Cambridge University Press

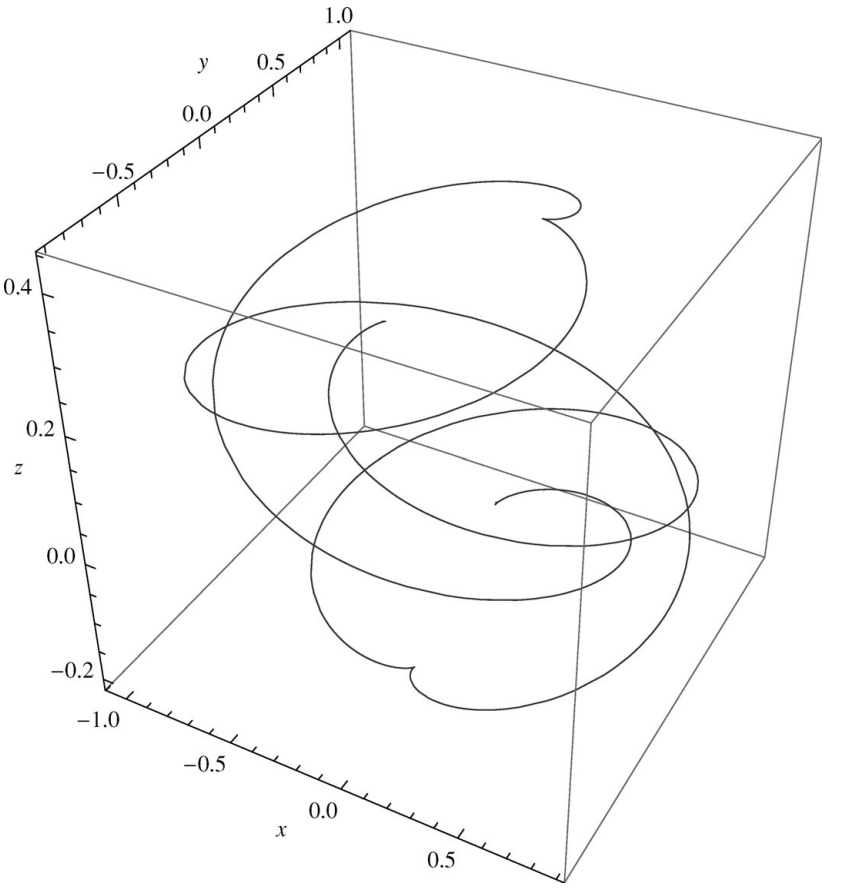


**Figure 7.** Field line for the non-centered simple Alfvén wave (5.19) for $k_0 = 200$, $r_0 = 1$ and $0 < \varphi < 3\pi/c_0$. The field line has cusps when the field line intersects the current sheet. The cusps occur at $\varphi = (\varphi_c + n\pi)/c_0$, where $\varphi_c = 5.0424^\circ$ (see (5.52)).

The choice $\Theta_0 = \pi/4$, yields the solution

$$\alpha = \varphi, \quad \beta = \varphi, \quad \Phi = 3\varphi - \frac{\pi}{2}, \quad \Theta_0 = \frac{\pi}{4}. \tag{5.62}$$

*5.4. Serret–Frenet equations*

An alternative approach to constructing Alfvén simple waves is to specify the wave normal **n** and then solve (5.5) for $\mathbf{B}(\varphi)$. Using (3.36) in (5.5), the equations for the magnetic field **B** in the Serret–Frenet frame base reduces to the equations

$$\frac{dB_1}{d\varphi} - \kappa B_2 = 0,$$

$$\frac{dB_2}{d\varphi} + \kappa B_1 - \tau B_3 = -\alpha(\varphi) B_3,$$

$$\frac{dB_3}{d\varphi} + \tau B_2 = \alpha(\varphi) B_2, \tag{5.63}$$

https://doi.org/10.1017/S0022377809990596 Published online by Cambridge University Press

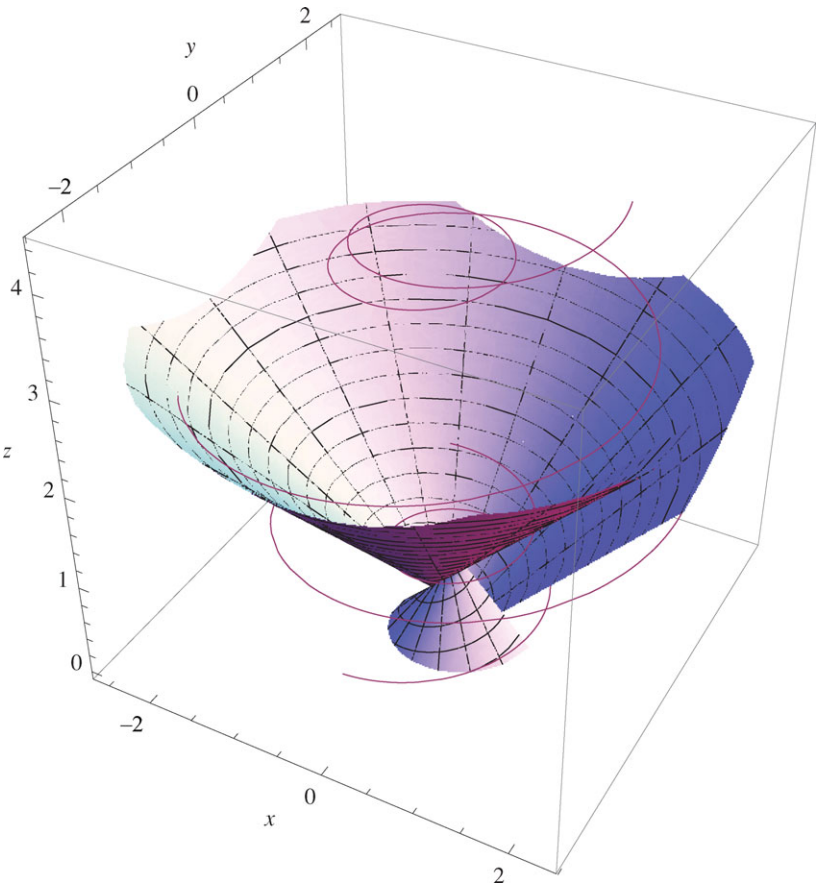


**Figure 8.** (Color online) Field line and current sheet for the non-centered simple Alfvén wave (5.19) for $k_0 = 10$, $r_0 = 1$, and $0 < \varphi < 3\pi/c_0$. The field line in this case does not hit the singular current surface.

where $\kappa(\varphi)$ and $\tau(\varphi)$ are the curvature and torsion coefficients of the curve $\mathbf{X}(\varphi)$ in the Serret–Frenet base. The dimensionless function $\alpha(\varphi)$ is the proportionality factor relating $\mathbf{B}'(\varphi)$ to $\mathbf{n} \times \mathbf{B}$ in the Alfvén eigenequation (5.5).

Equations (5.63) can be rewritten in the Serret–Frenet form:

$$\frac{du}{d\varphi} - \kappa v = 0,$$

$$\frac{dv}{d\varphi} + \kappa u - \tilde{\tau} w = 0,$$

$$\frac{dw}{d\varphi} + \tilde{\tau} v = 0, \tag{5.64}$$

where

$$(u, v, w) = (B_1, B_2, B_3), \quad \tilde{\tau}(\varphi) = \tau(\varphi) - \alpha(\varphi). \tag{5.65}$$

Equations (5.64) are the Serret–Frenet equations (e.g., Eisenhart 1960) associated with the curve $\tilde{X}(\varphi)$ with curvature $\kappa(\varphi)$ and torsion $\tilde{\tau} = \tau(\varphi) - \alpha(\varphi)$ (i.e., in a

https://doi.org/10.1017/S0022377809990596 Published online by Cambridge University Press

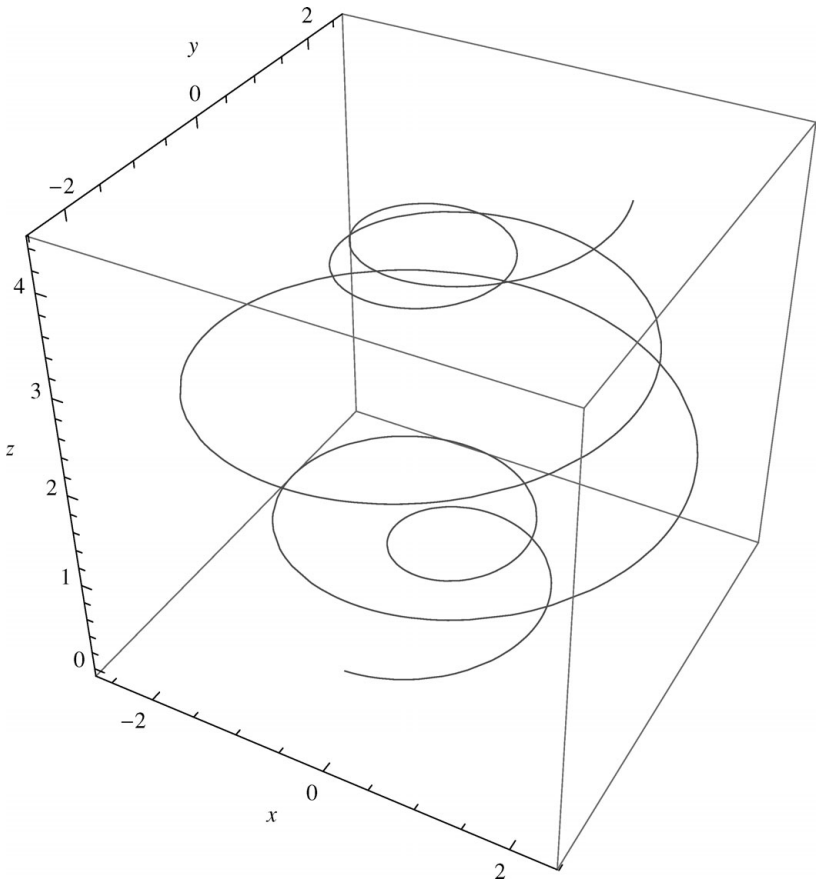


**Figure 9.** Field line for the non-centered simple Alfvén wave (5.19) for $k_0 = 10$, $r_0 = 1$, and $0 < \varphi < 3\pi/c_0$. The field line in this case does not hit the singular current surface.

fixed Cartesian coordinate base, the $i$th components of $\mathbf{e}_1, \mathbf{e}_2, \mathbf{e}_3$, namely $(u, v, w) = (e_1^i, e_2^i, e_3^i)$ for $i = 1, 2, 3$ satisfy (5.64)). The Serret–Frenet equations (5.64) have integral $u^2 + v^2 + w^2 = const.$ (i.e., $B^2 = const.$). Without loss of generality we may choose $(u, v, w) = \mathbf{e}_B$ to be the unit vector along the magnetic field.

Equations (5.64) may be reduced to a linear, second-order differential equation, by means of a stereographic projection of $(u, v, w)$ from the unit two-sphere $S^2$: $u^2 + v^2 + w^2 = 1$ onto the $(u, v)$ plane $R^2$, to obtain a Ricatti equation, which reduces to a second-order linear ordinary differential equation by means of a Cole–Hopf transformation (see, e.g., Eisenhart 1960). To be specific, consider the projection of the point $P = (u, v, w)$ on $S^2$ from the north pole $N = (0, 0, 1)$ by the straight line $NP$ intersecting the $(u, v)$ plane at the point $(u', v')$, where

$$u' = \frac{u}{1 - w}, \quad v' = \frac{v}{1 - w}, \quad u^2 + v^2 + w^2 = 1. \tag{5.66}$$

From (5.66),

$$u'^2 + v'^2 = \frac{1 + w}{1 - w}, \quad w = \frac{u'^2 + v'^2 - 1}{u'^2 + v'^2 + 1}. \tag{5.67}$$

https://doi.org/10.1017/S0022377809990596 Published online by Cambridge University Press

The inverse of the transformations (5.66) are

$$u = \frac{2u'}{u'^2 + v'^2 + 1}, \quad v = \frac{2v'}{u'^2 + v'^2 + 1}, \quad w = \frac{u'^2 + v'^2 - 1}{u'^2 + v'^2 + 1}. \tag{5.68}$$

Using the transformations (5.66)–(5.68), and the Serret–Frenet equations (5.64) gives

$$\frac{du'}{d\varphi} = \kappa v' - \tilde{\tau} v' u', \quad \frac{dv'}{d\varphi} = -\kappa u' + \frac{1}{2}\tilde{\tau}(u'^2 - v'^2 - 1). \tag{5.69}$$

Introducing the complex quantity

$$\sigma = u' + iv', \tag{5.70}$$

(5.69) gives the Ricatti equation:

$$\frac{d\sigma}{d\varphi} = -i\kappa\sigma + \frac{i}{2}\tilde{\tau}(\sigma^2 - 1). \tag{5.71}$$

The Ricatti equation (5.71) can be linearized by the Cole–Hopf transformation:

$$\sigma = \frac{2i}{\tilde{\tau}}\frac{\dot{\Omega}}{\Omega}, \quad \dot{\Omega} = \frac{d\Omega}{d\varphi}, \tag{5.72}$$

to obtain the linear second-order ordinary differential equation (ODE):

$$\ddot{\Omega} + \dot{\Omega}\left(i\kappa - \frac{\tilde{\tau}_\varphi}{\tilde{\tau}}\right) + \frac{\tilde{\tau}^2}{4}\Omega = 0. \tag{5.73}$$

Thus, given the curvature coefficient $\kappa(\varphi)$ and torsion coefficient $\tilde{\tau}(\varphi) = \tau(\varphi) - \alpha(\varphi)$, the simple Alfvén eigenequations for $(B_1, B_2, B_3) = B(u, v, w)$ ($B = const.$), can be reduced to the linear second-order ODE (5.73). The sequence of transformations (5.66)–(5.73) for the Serret–Frenet equations were originally obtained by Darboux (see, e.g., Eisenhart 1960).

The implications of these transformations, is that solutions of (5.73) for given $\kappa(\varphi)$, $\tau(\varphi)$, and $\alpha(\varphi)$, give solutions of the Ricatti equation (5.71) for $\sigma = u' + iv'$. The inverse stereographic transformations (5.68) give solutions for $(u, v, w)$. In the present application $(u, v, w) = (B_1, B_2, B_3)/B$ and hence the procedure gives solutions for **B** for Alfvén simple waves.

**Example 1**

If $\kappa = const.$ and $\tilde{\tau} = const.$ (5.73) has general solution

$$\Omega = a_1 \exp(i\lambda_1\varphi) + a_2 \exp(i\lambda_2\varphi), \tag{5.74}$$

where

$$\lambda_{1,2} = \frac{1}{2}(-\kappa \pm \tilde{K}), \quad \tilde{K} = \sqrt{\kappa^2 + \tilde{\tau}^2}. \tag{5.75}$$

One can obtain solutions for $(u, v, w)$ using the transformations (5.66)–(5.73). This is a complicated procedure. The general solution in this case is more easily obtained directly from (5.64). The solution of (5.64) can be written in the form

$$\begin{aligned}(u, v, w) = &(\cos\alpha_0 \sin\beta_0, 0, \sin\alpha_0 \sin\beta_0) \\ &+ \cos\beta_0(\sin\alpha_0 \sin\varphi_B, \cos\varphi_B, -\cos\alpha_0 \sin\varphi_B),\end{aligned} \tag{5.76}$$

https://doi.org/10.1017/S0022377809990596 Published online by Cambridge University Press

where

$$\kappa_B \equiv \kappa = \frac{\sin\alpha_0}{R_B}, \quad \tau_B \equiv \tilde{\tau} = \frac{\cos\alpha_0}{R_B},$$
$$K_B = \sqrt{\kappa_B^2 + \tau_B^2} = \frac{1}{R_B}, \quad \varphi_B = \frac{\varphi}{R_B}. \tag{5.77}$$

In (5.77) we have introduced subscripts $B$ to emphasize, that the torsion coefficient of the curve $X(\varphi)$ is in general different that the torsion coefficient for the corresponding curve for $(B_1, B_2, B_3)$ (see 5.65)). In (5.76) one can replace $\varphi_B$ by $\varphi_B + \delta$ if desired. The solution (5.76) also satisfies the equations:

$$u^2 + v^2 + w^2 = u_0^2 + v_0^2 + w_0^2 = 1, \quad \kappa_B u_0 - \tau_B w_0 = 0, \tag{5.78}$$

where $(u_0, v_0, w_0)$ is the value of $(u, v, w)$ at $\varphi_B = 0$. From (5.76) we find

$$u\cos\alpha_0 + w\sin\alpha_0 = \sin\beta_0. \tag{5.79}$$

Thus, the solution (5.76) for $(u, v, w)$ is a curve on the unit sphere, where the plane (5.79) intersects the sphere.

To complete the specification of the simple wave solution requires the specification of $f(\varphi)$ defining the wave phase $\varphi$ and also requires specification of the space curve $\mathbf{X}(\varphi)$ with unit tangent vector $\mathbf{e}_1 = \mathbf{n}(\varphi) = \mathbf{X}'(\varphi)/|\mathbf{X}'(\varphi)|$, with curvature $\kappa$ and torsion $\tau = \tilde{\tau} + \alpha(\varphi)$. For the sake of simplicity, we consider the case $\alpha = \alpha(\varphi) = const.$, for which

$$\mathbf{X}(\varphi) = R_X\,(\sin\Theta_0\sin\varphi_X, -\sin\Theta_0\cos\varphi_X, \cos\Theta_0\varphi_X)\,,$$
$$\mathbf{e}_1 = (\sin\Theta_0\cos\varphi_X, \sin\Theta_0\sin\varphi_X, \cos\Theta_0)\,,$$
$$\mathbf{e}_2 = (-\sin\varphi_X, \cos\varphi_X, 0)\,,$$
$$\mathbf{e}_3 = (-\cos\Theta_0\cos\varphi_X, -\cos\Theta_0\sin\varphi_X, \sin\Theta_0)\,. \tag{5.80}$$

In (5.80),

$$\varphi_X = \frac{\varphi}{R_X}, \quad K_X = \sqrt{\kappa_X^2 + \tau_X^2} = \frac{1}{R_X},$$
$$\kappa_X = \frac{\sin\Theta_0}{R_X} \equiv \frac{\sin\alpha_0}{R_B}, \quad \tau_X = \frac{\cos\Theta_0}{R_X}. \tag{5.81}$$

Note that the curvature $\kappa_B = \kappa_X$ but $\tau_B \neq \tau_X$ (note $\tau_B = \tau_X - \alpha$: see (5.65)).

*Examples*

In the following analysis, we set $R_B = 1$ and $R_X$ is a free parameter. The solutions turn out to depend on the parameter $R_X/R_B$, which roughly describes the torsion of the magnetic field (we set $\tau_X = 0$ in the examples).

Consider the class of simple waves described by (5.76)–(5.81). The field line equations (3.30) for the case of non-centered waves with $f(\varphi) = \varphi/k_0$ reduce to

$$\frac{d\tilde{q}_2}{d\varphi} = -\kappa_X\frac{B_2}{B_1}\tilde{q}_2 + \tau_X\tilde{q}_3 + \frac{1}{k_0}\left(\frac{B_2}{B_1} - \kappa_X\varphi\right),$$
$$\frac{d\tilde{q}_3}{d\varphi} = -\tilde{q}_2\left(\tau_X + \kappa_X\frac{B_3}{B_1}\right) + \frac{1}{k_0}\left(\frac{B_3}{B_1}\right), \tag{5.82}$$

where $(B_1, B_2, B_3) = |B|(u, v, w)$ is given by (5.76).

https://doi.org/10.1017/S0022377809990596 Published online by Cambridge University Press

*Centered waves with $k_0 \to \infty$*

We further restrict our attention to simple waves with $\tau_X = 0$ (i.e., $\Theta_0 = \pi/2$) and with $k_0 \to \infty$ (i.e to centered waves). For this class of waves, the moving tri-hedron $(\mathbf{e}_1, \mathbf{e}_2, \mathbf{e}_3)$ is given by

$$\mathbf{e}_1 = (\cos\varphi_X, \sin\varphi_X, 0), \quad \mathbf{e}_2 = (-\sin\varphi_X, \cos\varphi_X, 0), \quad \mathbf{e}_3 = (0, 0, 1). \tag{5.83}$$

The solution for the magnetic field from (5.76) has the form

$$B_1 = B(a + b\sin\varphi_B), \quad B_2 = B\cos\beta_0\cos\varphi_B, \quad B_3 = B(c - d\sin\varphi_B), \tag{5.84}$$

where

$$a = \cos\alpha_0\sin\beta_0, \quad b = \cos\beta_0\sin\alpha_0, \quad c = \sin\alpha_0\sin\beta_0, \quad d = \cos\alpha_0\cos\beta_0. \tag{5.85}$$

For $\Theta_0 = \pi/2$ and $k_0 \to \infty$ the wave phase $\varphi_X = \varphi/R_X$ satisfies the wave front equation:

$$G \equiv -(\tilde{x}\cos\varphi_X + \tilde{y}\sin\varphi_X) = 0. \tag{5.86}$$

This class of solutions has a current singularity on the $\tilde{z}$-axis as $\tilde{r} = (\tilde{x}^2 + \tilde{y}^2)^{1/2} \to 0$, where $|\nabla\varphi_B| = 1/F \to \infty$ (see (5.23) et seq.). There are two scale lengths for the wave: $R_X$ and $R_B$ associated with the curve $\mathbf{X}(\varphi)$ used to describe the wave front and the magnetic field, respectively. The field line equations (5.82) in this limit reduce to

$$\frac{d\tilde{q}_2}{d\varphi} + \kappa_X\left(\frac{B_2}{B_1}\right)\tilde{q}_2 = 0, \quad \frac{d\tilde{q}_3}{d\varphi} = -\kappa_X\frac{B_3}{B_1}\tilde{q}_2. \tag{5.87}$$

Equations (5.87) have solutions for $\tilde{q}_2$ and $\tilde{q}_3$ of the form

$$\tilde{q}_2 = \tilde{q}_{20}\frac{B_{10}}{B_1} = \tilde{q}_{20}\frac{a}{a + b\sin\varphi_B}, \quad \tilde{q}_3 = \tilde{q}_{30} - \tilde{q}_{20}a\sin\alpha_0 I_1, \tag{5.88}$$

where

$$I_1 = \int_0^{\varphi_B}\frac{(c - d\sin\varphi)}{(a + b\sin\varphi)^2}d\varphi. \tag{5.89}$$

The integral (5.89) for $|a| > |b|$ can be expressed in the form

$$I_1 = \left[\frac{2(ac + bd)}{\sqrt{a^2 - b^2}}\left(\mathrm{Arctan}\left(\frac{b + a\tau}{\sqrt{a^2 - b^2}}\right) + w(\varphi)\right) + \frac{(bc + ad)\cos\varphi}{(a + b\sin\varphi)}\right]_{\varphi=0}^{\varphi=\varphi_B}, \tag{5.90}$$

where

$$\tau(\varphi) = \tan\left(\frac{\varphi}{2}\right), \quad w(\varphi) = \left[\frac{\varphi + \pi}{2\pi}\right]\pi. \tag{5.91}$$

In (5.91) the square bracket notation $[x]$ means the integer part of $x$. The Arctan$(x)$ function in (5.91) denotes the principal branch of Arctan$(x)$ which is defined for $|x| \leqslant \pi/2$. In the evaluation of the formula (5.90) for $I_1$, use of (5.85) gives

$$a^2 - b^2 = \sin(\beta_0 - \alpha_0)\sin(\beta_0 + \alpha_0), \quad bc + ad = \frac{1}{2}\sin(2\beta_0), \quad ac + bd = \frac{1}{2}\sin(2\alpha_0), \tag{5.92}$$

for $a^2 - b^2$, $bc + ad$ and $ac + bd$ in (5.90). The field lines for the simple wave using $(\tilde{x}, \tilde{y}, \tilde{z})$ coordinates are given by

$$\tilde{x} = -\tilde{q}_2\sin\varphi_X, \quad \tilde{y} = \tilde{q}_2\cos\varphi_X, \quad \tilde{z} = \tilde{q}_3. \tag{5.93}$$

https://doi.org/10.1017/S0022377809990596 Published online by Cambridge University Press

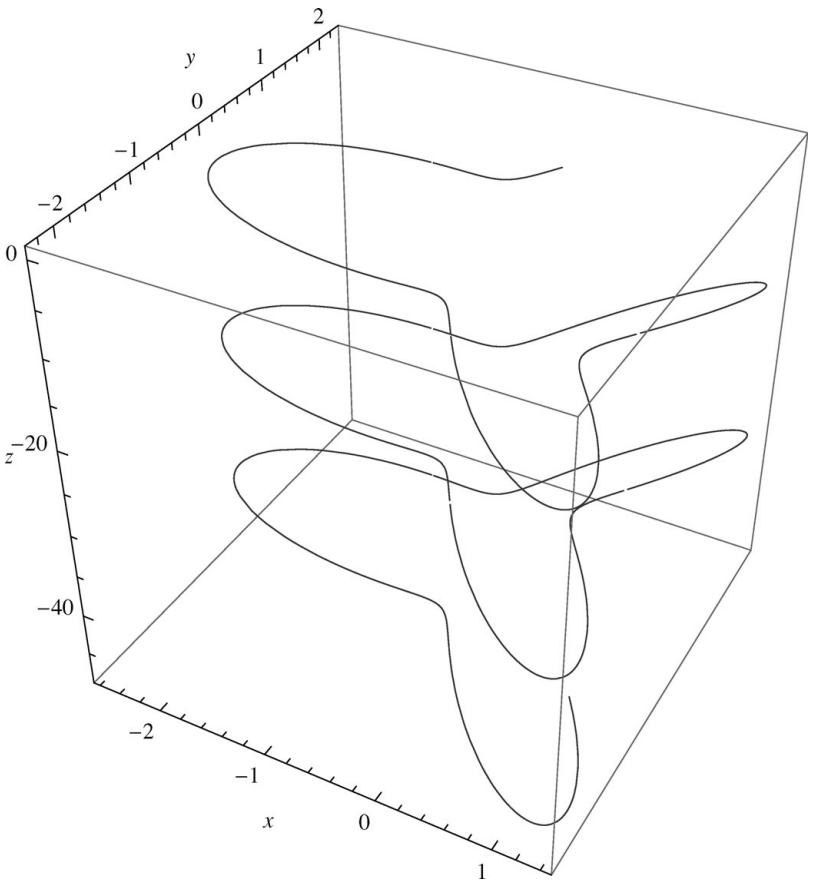


**Figure 10.** A field line for a centered simple Alfvén wave (5.83)–(5.85) which generalizes Barnes (1976) solution. The solution couples the evolution of the wave front, with scale $R_X$ to the magnetic field geometry in the Serret–Frenet frame, with scale $R_B$. The field lines are given by (5.93). The parameters are $R_X = 3$, $R_B = 1$, $\beta_0 = 30°$, $|B| = 1$, $q_{30} = 0$, $q_{20} = 1$.

Figure 10 shows a field line (5.93) for the simple wave (5.80)–(5.86), for the parameter values:

$$R_B = 1, \quad R_X = 3, \quad \beta_0 = \frac{\pi}{6}, \quad B = 1, \quad \alpha_0 = \text{Arcsin}\left(\frac{R_B}{R_X}\right) = 0.339837. \qquad (5.94)$$

The field line is a distorted helix, with axis of symmetry, roughly along the $\tilde{z}$-axis (there are two fat lobes, and one thin lobe for each period along the $\tilde{z}$ direction). The parameters $q_{20} = 1$ and $q_{30} = 0$ for this field line. The parametric form $[\tilde{x}(\varphi), \tilde{y}(\varphi), \tilde{z}(\varphi)]$ of the field line is displayed in Fig. 11. The $\tilde{x}(\varphi)$ and $\tilde{y}(\varphi)$ profiles are periodic in $\varphi$, but $\tilde{z}(\varphi)$ is monotonic decreasing with a smooth step-like structure.

Figure 12 shows a field line for the same parameters as in Fig. 10, except that $R_B = 1$ and $R_X = 10$. Note the small-scale loops associated with the torsion of the magnetic field $(B_1, B_2, B_3)$ components, superimposed on a large-scale helical structure associated with the curve $\mathbf{X}(\varphi)$ with wave normal $\mathbf{n}(\varphi)$. The field is directed downward in the negative $\tilde{z}$ direction. The parametric dependence of the field lines

https://doi.org/10.1017/S0022377809990596 Published online by Cambridge University Press

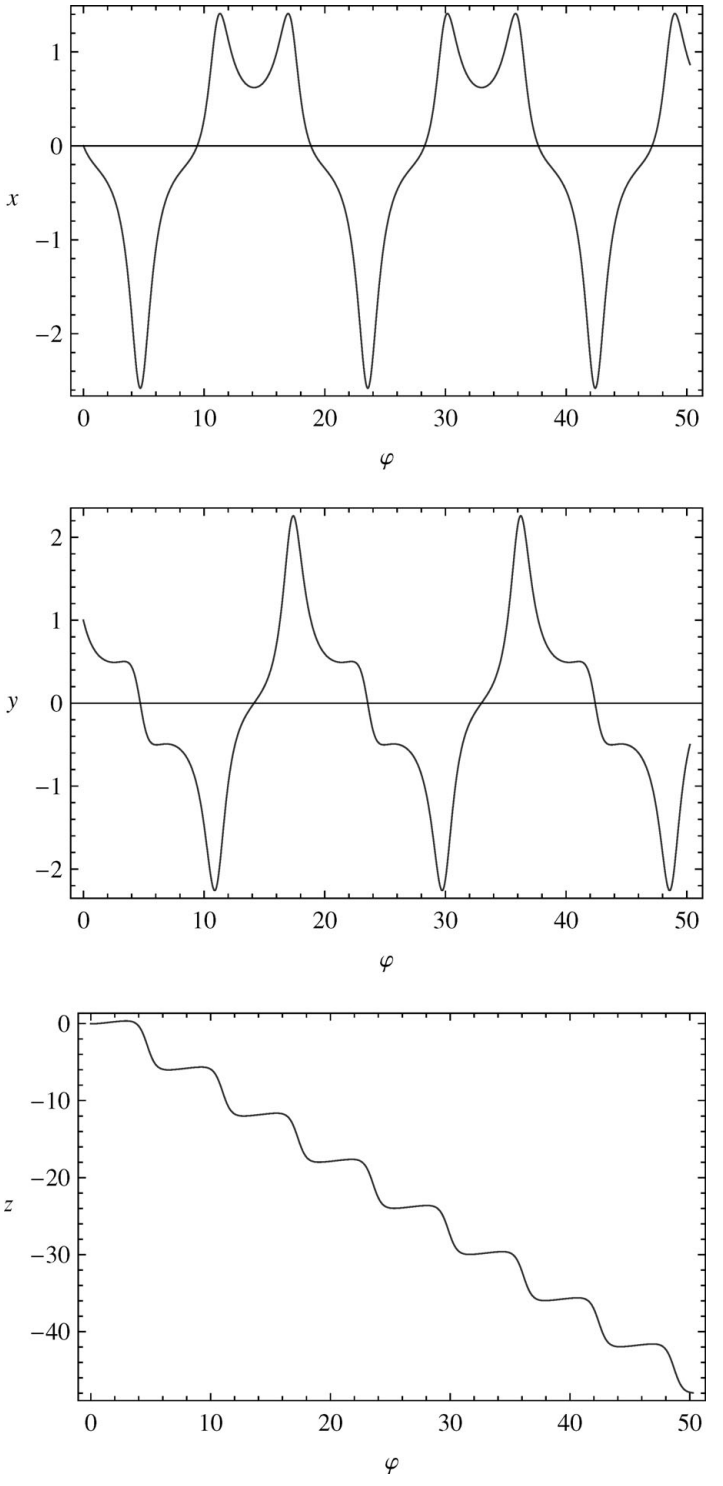


**Figure 11.** The field line $[\tilde{x}(\varphi), \tilde{y}(\varphi), \tilde{z}(\varphi)]$ versus $\varphi$, for $R_B = 1$ and $R_X = 3$ corresponding to the field line in Fig. 10.

https://doi.org/10.1017/S0022377809990596 Published online by Cambridge University Press

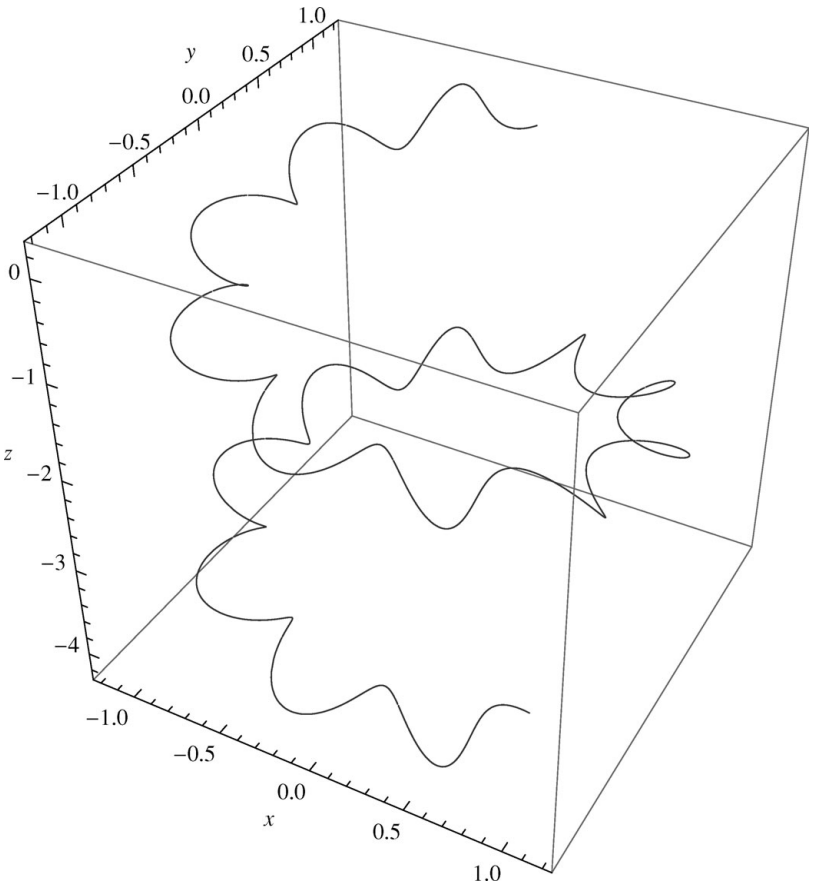


**Figure 12.** A field line for the simple wave (5.83)–(5.85), with field lines (5.93). Same parameters as in Fig. 10, except $R_B = 1$ and $R_X = 10$.

$[\tilde{x}(\varphi), \tilde{y}(\varphi), \tilde{z}(\varphi)]$ on $\varphi \equiv \varphi_B$ (note $R_B = 1$) is exhibited in Fig. 13 ($\varphi$ is measured in radians). The $\tilde{x}$ and $\tilde{y}$ components exhibit a large-scale periodic motion, whereas $\tilde{z}$ decreases monotonically on the large scale. Small-scale variations associated with $R_B$ are superimposed on the large-scale structure.

Figure 14 shows a sample field line for the case $R_B = 1$ and $R_X = 4000$. The field line is a spiral with axis parallel to the $x$-axis. In the limit as $R_X \to \infty$, $b = c = 0$, $a = \sin\beta_0$, $d = \cos\beta_0$, and the solution depends only on $\varphi = \varphi_B$, and the wave normal $\mathbf{n} = (1, 0, 0)$. These features of the solution are illustrated in Fig. 14.

Other numerical examples of simple Alfvén waves can clearly be constructed by the above methods. Below we discuss two more examples, but refrain from a detailed numerical investigation of the solutions.

**Example 2**

For the case

$$\kappa(\varphi) = a_0 + b_0 \tanh\varphi, \quad \tilde{\tau}(\varphi) = k\ \mathrm{sech}\varphi, \tag{5.95}$$

(5.73) for $\Omega$ reduces to the equation:

$$(1 - w^2)\frac{d^2\Omega}{dw^2} + \frac{d\Omega}{dw}[i(a_0 + b_0 w) - w] + \frac{k^2}{4}\Omega = 0, \tag{5.96}$$

https://doi.org/10.1017/S0022377809990596 Published online by Cambridge University Press

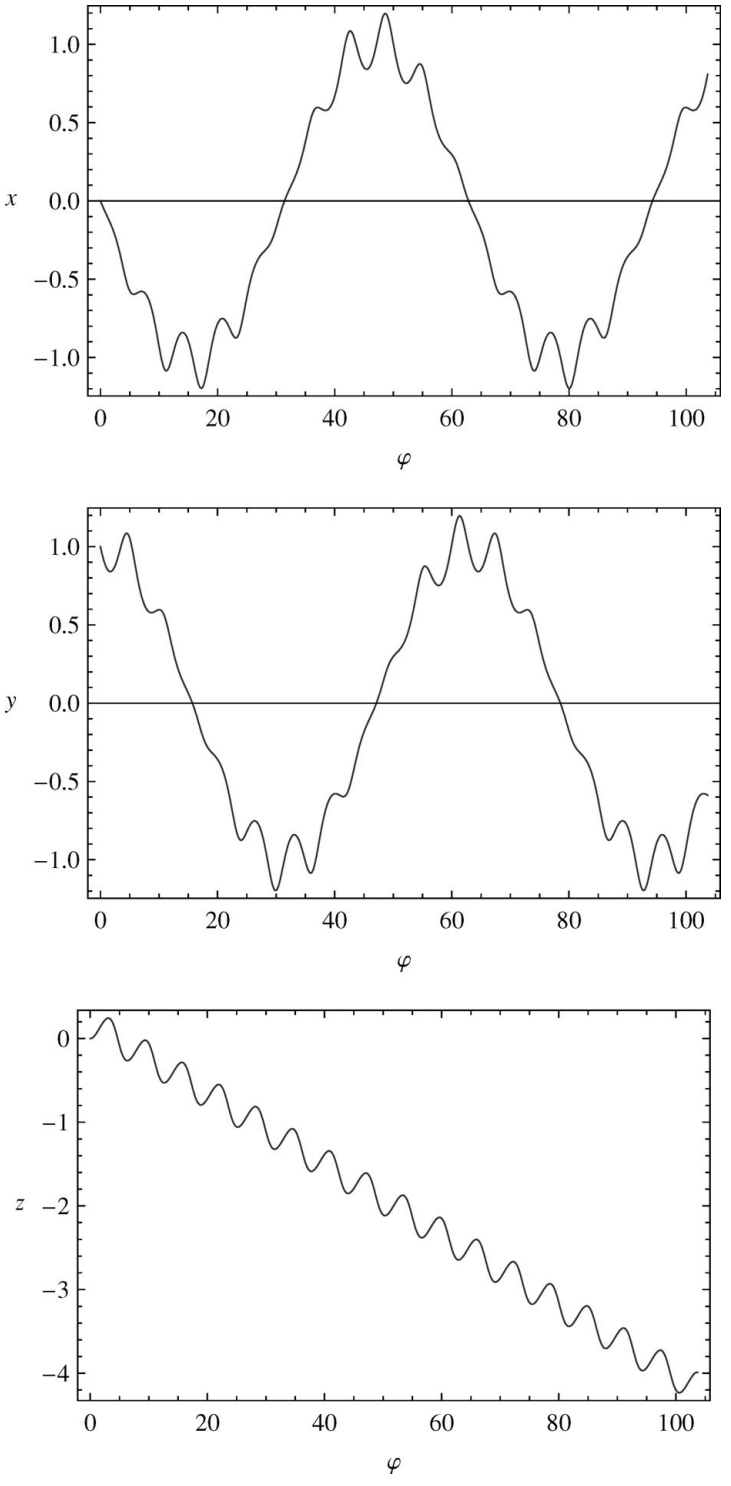


**Figure 13.** Parametric form of the field line $[\tilde{x}(\varphi), \tilde{y}(\varphi), \tilde{z}(\varphi)]$ of Fig. 12, versus $\varphi$, for $R_B = 1$ and $R_X = 10$.

https://doi.org/10.1017/S0022377809990596 Published online by Cambridge University Press

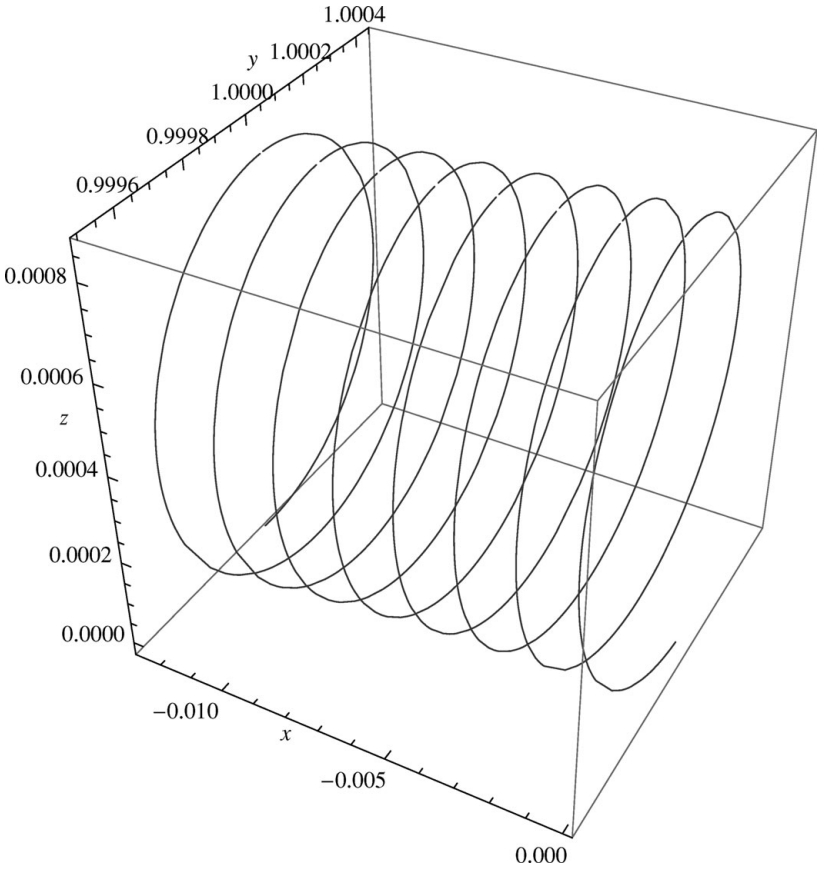


**Figure 14.** Field line for the simple wave described by (5.83)–(5.85) and (5.93). Same parameters as in Fig. 10, except $R_B = 1$ and $R_X = 4000$.

where

$$w = \tanh\varphi, \tag{5.97}$$

Note that $\kappa(\varphi)$ and $\tilde{\tau}(\varphi)$ are bounded for real $\varphi$. Equation (5.96) can be reduced to the hypergeometric equation:

$$z(1-z)\frac{d^2\Omega}{dz^2} + [c - z(1+a+b)]\frac{d\Omega}{dz} - ab\Omega = 0, \tag{5.98}$$

where

$$z = \frac{1}{2}(1+w), \quad w = \tanh\varphi,$$
$$a = \frac{1}{2}\left[-ib_0 - \sqrt{k^2 - b_0^2}\right], \quad b = \frac{1}{2}\left[-ib_0 + \sqrt{k^2 - b_0^2}\right],$$
$$c = \frac{1}{2}\left[1 + i(a_0 - b_0)\right]. \tag{5.99}$$

Equation (5.98) is satisfied by Gauss's hypergeometric function ${}_2F_1(a,b,c,z)$ (see, e.g., Abramowitz and Stegun 1965, Chapter 15, p. 556). Polynomial solutions for for

https://doi.org/10.1017/S0022377809990596 Published online by Cambridge University Press

$\Omega$ result if $b_0 = 0$ and $k = 2n$ where $n$ is an integer. This case corresponds to a constant curvature coefficient $\kappa$ and a variable torsion $\tilde{\tau}(\varphi)$.

**Example 3**

For the choice

$$\kappa(\varphi) = \frac{(I_2 - I_3)}{I_2 I_3} B_3, \quad \tilde{\tau}(\varphi) = \frac{(I_2 - I_1)}{I_2 I_1} B_1, \tag{5.100}$$

the Serret–Frenet equations (5.64) for $(u, v, w) = (B_1, B_2, B_3)$ reduce to Euler's equations:

$$\begin{aligned} \frac{dB_1}{d\varphi} &= \frac{(I_2 - I_3)}{I_2 I_3} B_2 B_3, \\ \frac{dB_2}{d\varphi} &= \frac{(I_3 - I_1)}{I_3 I_1} B_3 B_1, \\ \frac{dB_3}{d\varphi} &= \frac{(I_1 - I_2)}{I_1 I_2} B_1 B_2 \end{aligned} \tag{5.101}$$

for rigid body rotational dynamics, where $I_1$, $I_2$, and $I_3$ are analogous to the principal moments of inertia and $(B_1, B_2, B_3)$ are analogous to the angular momenta $(\Pi_1, \Pi_2, \Pi_3)$ about the principal axes (i.e., $\Pi_j = I_j \Omega_j$ where $\Omega_j$ is the angular velocity about the $j$th principal axis). The Euler–Poincaré form and Hamiltonian form of the Euler equations are discussed, for example, by Marsden and Ratiu (1994) and by Holm et al. (1998). Analytical solutions of Euler's equations in terms of Jacobian elliptic functions are listed in Marsden and Ratiu (1994).

## 6. Summary and discussion

In this paper, we have obtained examples of simple Alfvén waves, using Boillat's formalism (Boillat 1970) for multi-dimensional simple waves, thus extending the previous examples obtained by Barnes (1976) and Webb et al. (1995).

MHD simple waves were obtained by requiring that the MHD state vector $\mathbf{W} = (\rho, \mathbf{u}^T, \mathbf{B}^T, p)^T$ be purely a function of the wave phase $\varphi(x, y, z, t)$. This condition implies that $d\mathbf{W}/d\varphi$ is a right eigenvector of the MHD matrix eigensystem (3.5), and that the wave normal $\mathbf{n}(\varphi)$ and the eigenvalue $\lambda(\varphi)$ of the mode of interest should be solely functions of $\varphi$. The latter two conditions on $\lambda(\varphi)$ and $\mathbf{n}(\varphi)$ imply that $\varphi$ is given implicitly by the equation: $f(\varphi) = \mathbf{r} \cdot \mathbf{n}(\varphi) - \lambda(\varphi) t$ (see (3.9)), where $f(\varphi)$ is an arbitrary function of $\varphi$. Solutions with $f(\varphi) = 0$ are known as centered waves whereas solutions with $f(\varphi)$ a non-zero function of $\varphi$ are known as non-centered waves.

The 1D simple Alfvén wave propagating along the $z$-axis in standard textbooks (e.g., Cabannes 1970) is obtained by using the ansatz $f(\varphi) = \varphi/k_0$ for $f(\varphi)$ where $k_0$ is a characteristic wave number and by setting and $\mathbf{n} = (0, 0, 1)$. Field lines for the wave are helices, winding about the direction of propagation (see Fig. 1). More general 1D planar solutions are obtained for other choices of $f(\varphi)$. The Barnes simple Alfvén wave in this scheme is obtained by setting $f(\varphi) = 0$, and by setting $\mathbf{n}(\varphi) = (\cos\varphi, \sin\varphi, 0)$ (see, e.g., Barnes 1976 and Fig. 2). The magnetic field lines and the wave normal are concentric circles centered on the $z$-axis, and lying in $z = const.$ planes. The current in the wave $\mathbf{J} = \nabla \times \mathbf{B}/\mu$ is directed along the $z$ direction and diverges on the $z$-axis as $1/r$ as $r = (x^2 + y^2)^{1/2} \to 0$. The current blow-up on the $z$-axis is an example of wave breaking for Alfvén simple waves. The Barnes solution (Barnes 1976) has $f(\varphi) = 0$ and is an example of a centered simple wave.

https://doi.org/10.1017/S0022377809990596 Published online by Cambridge University Press

The Barnes solution can be generalized by allowing the magnetic field to have a non-zero constant component along the $z$-axis, but still maintaining $\mathbf{n}(\varphi) = (\cos\varphi, \sin\varphi, 0)$ for the wave normal. This results in a simple wave with helical field lines, which have the same form as the 1D planar, non-centered simple Alfvén wave as illustrated in Fig. 1. However, this solution (described in (5.29)–(5.30)) has a totally different current distribution and wave normal to the standard textbook simple Alfvén wave, with wave normal along the $z$-axis. The standard 1D planar simple wave has a wave normal directed along the $z$-axis, and a non-singular azimuthal current. The generalized Barnes solution (5.29)–(5.30) has an azimuthal wave normal, and the current is along the $z$-axis and diverges as $r = (\tilde{x}^2 + \tilde{y}^2)^{1/2} \to 0$. This example shows that two waves can have the same field lines, but have distinct wave normals and currents.

By allowing both the wave normal and the magnetic field to have non-zero and constant $z$ components, gives the centered simple wave obtained by Webb et al. (1995). The magnetic field lines then become generalized helices. The current in the wave now diverges on the cone $z = r\tan\Theta_0$. A typical field line (e.g., Fig. 3) starts on the current sheet (cone in $z > 0$ say) and ends on the current sheet in the other half plane. An inspection of the field line solutions reveals that the tangent vector to the field line $\mathbf{T} = d\mathbf{x}/d\varphi$ vanishes when the field line hits the current sheet (i.e., the field line has a cusp on the current sheet, where the wave breaks: see Figs. 4 and 5). The Barnes simple wave solution is obtained in the limit that $\Theta_0 \to \pi/2$ and with zero $z$ components for $\mathbf{n}(\varphi)$ and $\mathbf{B}$. In this limit, the cone current sheet collapses onto the $\tilde{z}$-axis.

The centered simple Alfvén solution of Webb et al. (1995) can be generalized to the case of a non-centered wave for which $f(\varphi) = \varphi/k_0$ (see (5.19) and Figs. 6–9). In this case, the current sheet cone is a distorted conical surface which does not join back up with itself. There are two types of field lines: those that intersect the current sheet (Figs. 6 and 7) and those that do not (e.g., Fig. 9). The latter type of field line has a helical structure of varying diameter, and resembles a pig's curly tail.

The above examples were constructed by first specifying the wave normal $\mathbf{n}(\varphi)$ and then determining solutions for $\mathbf{B}(\varphi)$ consistent with the requirement $\mathbf{n}\cdot d\mathbf{B}/d\varphi = 0$, or by specifying $\mathbf{B}(\varphi)$ and then determining $\mathbf{n}(\varphi)$, using rectangular Cartesian coordinates in the group velocity frame of the wave. The magnetic field lines for the wave were then integrated using the Serret–Frenet formulation. An alternative approach is to solve the eigenequations $d\mathbf{B}/d\varphi = \alpha(\varphi)\mathbf{n}(\varphi)\times\mathbf{B}(\varphi)$ using the Serret–Frenet formalism. This approach gives rise to a more complex family of Alfvén simple waves (Figs. 10–14). The more complicated nature of these waves arises because there are two sets of curvature and torsion coefficients describing the simple wave associated with the curve $\mathbf{X}(\varphi)$ used to define the wave normal $\mathbf{n}(\varphi)$ and also the equations describing the magnetic field in the Serret–Frenet frame. Field lines with finger like protuberances superimposed on a basic helical structure (Fig. 10), helical fields with smaller scale loops superimposed (Fig. 12) and helical structures (Fig. 14) were obtained.

The Serret–Frenet equations for $\mathbf{B}$ were mapped by stereographic projection from the two-sphere $S^2$ to the 2D $(u, v)$ plane $R^2$, resulting in a Ricatti equation for the transformed variable $\sigma = u' + iv'$, which in turn was linearized by a Cole–Hopf transformation (this complicated transformation is originally due to Darboux (see Eisenhart 1960). The main point is, that these transformations may be used to generate simple Alfvén wave solutions. For a judicious choice of the curvature and

https://doi.org/10.1017/S0022377809990596 Published online by Cambridge University Press

torsion coefficients, the Serret–Frenet equations reduce to the Euler equations of rigid body dynamics, with known solutions in terms of Jacobian elliptic functions (e.g., Marsden and Ratiu 1994).

It is of interest to study the magnetic helicity of the Alfvén wave solutions presented in the present paper (e.g., Berger and Field 1984; Berger and Prior 2006). However, this investigation lies beyond the scope of the present paper.

*Acknowledgements*

G. M. Webb and G. P. Zank were supported in part by NASA grants NN05GG83G and NSF grant nos. ATM-03-17509 and ATM-04-28880. R. Ratkiewicz acknowledges support from the Polish Ministry of Science and Higher Education (PMSHE)-Grant N N203 4159 33.

## Appendix A

In this appendix we list the matrices $\mathbf{A}^{(i)}$ $\{1 \leqslant i \leqslant 3\}$ for the conservative MHD system based on (2.1)–(2.4), corresponding to the $x$, $y$, and $z$ derivative operators in (3.1) using the primitive MHD variables (3.2). The matrices $\mathbf{A}^{(i)}$ are

$$\mathbf{A}^{(1)} = \begin{pmatrix} u_x & \rho & 0 & 0 & 0 & 0 & 0 & 0 \\ 0 & u_x & 0 & 0 & -\frac{B_x}{\mu\rho} & \frac{B_y}{\mu\rho} & \frac{B_z}{\mu\rho} & \frac{1}{\rho} \\ 0 & 0 & u_x & 0 & -\frac{B_y}{\mu\rho} & -\frac{B_x}{\mu\rho} & 0 & 0 \\ 0 & 0 & 0 & u_x & -\frac{B_z}{\mu\rho} & 0 & -\frac{B_x}{\mu\rho} & 0 \\ 0 & 0 & 0 & 0 & u_x & 0 & 0 & 0 \\ 0 & B_y & -B_x & 0 & 0 & u_x & 0 & 0 \\ 0 & B_z & 0 & -B_x & 0 & 0 & u_x & 0 \\ 0 & A & 0 & 0 & 0 & 0 & 0 & u_x \end{pmatrix}, \tag{A 1}$$

$$\mathbf{A}^{(2)} = \begin{pmatrix} u_y & 0 & \rho & 0 & 0 & 0 & 0 & 0 \\ 0 & u_y & 0 & 0 & -\frac{B_y}{\mu\rho} & -\frac{B_x}{\mu\rho} & 0 & 0 \\ 0 & 0 & u_y & 0 & \frac{B_x}{\mu\rho} & -\frac{B_y}{\mu\rho} & \frac{B_z}{\mu\rho} & \frac{1}{\rho} \\ 0 & 0 & 0 & u_y & 0 & -\frac{B_z}{\mu\rho} & -\frac{B_y}{\mu\rho} & 0 \\ 0 & -B_y & B_x & 0 & u_y & 0 & 0 & 0 \\ 0 & 0 & 0 & 0 & 0 & u_y & 0 & 0 \\ 0 & 0 & B_z & -B_y & 0 & 0 & u_y & 0 \\ 0 & A & 0 & 0 & 0 & 0 & 0 & u_y \end{pmatrix}, \tag{A 2}$$

https://doi.org/10.1017/S0022377809990596 Published online by Cambridge University Press

$$\mathbf{A}^{(3)} = \begin{pmatrix} u_z & 0 & 0 & \rho & 0 & 0 & 0 & 0 \\ 0 & u_z & 0 & 0 & -\frac{B_z}{\mu\rho} & 0 & -\frac{B_x}{\mu\rho} & 0 \\ 0 & 0 & u_z & 0 & 0 & -\frac{B_z}{\mu\rho} & -\frac{B_y}{\mu\rho} & 0 \\ 0 & 0 & 0 & u_z & \frac{B_x}{\mu\rho} & \frac{B_y}{\mu\rho} & -\frac{B_z}{\mu\rho} & \frac{1}{\rho} \\ 0 & -B_z & 0 & B_x & u_z & 0 & 0 & 0 \\ 0 & 0 & -B_z & B_y & 0 & u_z & 0 & 0 \\ 0 & 0 & 0 & 0 & 0 & 0 & u_z & 0 \\ 0 & A & 0 & 0 & 0 & 0 & 0 & u_z \end{pmatrix}, \tag{A 3}$$

where $A = a^2\rho$ and $a$ is the adiabatic sound speed of the gas.

## Appendix B

It is instructive to write the eigensystem (3.5) for the right eigenvectors $\mathbf{R} = d\mathbf{W}/d\varphi$ using components perpendicular and parallel to $\mathbf{n}$ in the form

$$\tilde{u}_n\delta\rho + \rho\delta u_\parallel = 0, \tag{B 1}$$

$$\tilde{u}_n\delta u_\parallel + \frac{1}{\rho}\left(\delta p + \frac{\mathbf{B}_\perp\cdot\delta\mathbf{B}_\perp}{\mu} - \frac{B_n\delta B_\parallel}{\mu}\right) = 0, \tag{B 2}$$

$$\tilde{u}_n\delta\mathbf{u}_\perp - \frac{1}{\mu\rho}(B_n\delta\mathbf{B}_\perp + \mathbf{B}_\perp\delta B_\parallel) = 0, \tag{B 3}$$

$$\tilde{u}_n\delta B_\parallel = 0, \tag{B 4}$$

$$\tilde{u}_n\delta\mathbf{B}_\perp - B_n\delta\mathbf{u}_\perp + \mathbf{B}_\perp\delta u_\parallel = 0, \tag{B 5}$$

$$\tilde{u}_n\delta p + a^2\rho\delta u_\parallel = 0, \tag{B 6}$$

where

$$\tilde{u}_n = u_n - \lambda, \quad V_p = \lambda - u_n, \quad u_n = \mathbf{u}\cdot\mathbf{n}, \quad B_n = \mathbf{B}\cdot\mathbf{n},$$

$$\mathbf{u}_\perp = (\mathbf{I} - \mathbf{nn})\cdot\mathbf{u}, \quad \mathbf{B}_\perp = (\mathbf{I} - \mathbf{nn})\cdot\mathbf{B},$$

$$\delta u_\parallel = \mathbf{n}\cdot\frac{d\mathbf{u}}{d\varphi}, \quad \delta B_\parallel = \mathbf{n}\cdot\frac{d\mathbf{B}}{d\varphi},$$

$$\delta\mathbf{u}_\perp = (\mathbf{I} - \mathbf{nn})\cdot\frac{d\mathbf{u}}{d\varphi}, \quad \delta\mathbf{B}_\perp = (\mathbf{I} - \mathbf{nn})\cdot\frac{d\mathbf{B}}{d\varphi},$$

$$\delta\rho = \frac{d\rho}{d\varphi}, \quad \delta p = \frac{dp}{d\varphi}. \tag{B 7}$$

Equations (B 6) are the mass continuity (B 1), the parallel and perpendicular momentum (B 2)–(B 3), the parallel and perpendicular components of Faraday's (B 4)–(B 5), and the comoving gas energy (B 6).

https://doi.org/10.1017/S0022377809990596 Published online by Cambridge University Press

The right eigenvector $\mathbf{R} = d\mathbf{W}/d\varphi$ for the system (3.5) is given by

$$\mathbf{R} = \left(r_1, r_2, r_3, r_4, r_5, r_6, r_7, r_8\right)^T \equiv \left(\delta\rho, \delta u_{\parallel}, \delta\mathbf{u}_{\perp}^T, \delta B_{\parallel}, \delta\mathbf{B}_{\perp}^T, \delta p\right)^T. \tag{B 8}$$

For a non-trivial solution of (3.5) for $d\mathbf{W}/d\varphi \equiv \mathbf{R}$ (i.e., of (B 1)–(B 5)) it is necessary that $\lambda$ satisfy the eigenvalue equation

$$\det(\mathbf{A}_n - \lambda\mathbf{I}) \equiv \tilde{u}_n^2(\tilde{u}_n^2 - b_n^2)[\tilde{u}_n^4 - (b^2 + a^2)\tilde{u}_n^2 + b_n^2 a^2] = 0, \tag{B 9}$$

where

$$\tilde{u}_n = u_n - \lambda, \quad u_n = \mathbf{u}\cdot\mathbf{n}, \quad b_n = \mathbf{b}\cdot\mathbf{n}, \quad \mathbf{b} = \frac{\mathbf{B}}{(\mu_0\rho)^{1/2}}. \tag{B 10}$$

Here, $\tilde{u}_n$ denotes the component of the fluid velocity normal to the wave front in the wave frame, $\mathbf{b}$ is the Alfvén velocity, and $a$ is the gas sound speed. The solutions of the eigenvalue (B 9) for $\lambda$ are

$$\begin{aligned} &\lambda_1 = u_n - c_f, \quad \lambda_2 = u_n - b_n, \quad \lambda_3 = u_n - c_s, \quad \lambda_4 = u_n, \\ &\lambda_5 = u_n, \quad \lambda_6 = u_n + c_s, \quad \lambda_7 = u_n + b_n, \quad \lambda_8 = u_n + c_f, \end{aligned} \tag{B 11}$$

where

$$c_{f,s}^2 = \frac{1}{2}\{b^2 + a^2 \pm [(b^2 + a^2)^2 - 4b_n^2 a^2]^{1/2}\} \tag{B 12}$$

define the fast ($c_f$) and slow ($c_s$) magnetosonic speeds. The solutions (B 11) correspond to the backward and forward propagating magnetosonic waves ($\lambda_1$, $\lambda_3$, $\lambda_6$, $\lambda_8$), the backward and forward propagating Alfvén waves ($\lambda_2$, $\lambda_7$), the contact discontinuity of ordinary gas dynamics ($\lambda_4 = u_n$, $B_n \neq 0$, $\mathbf{u}' = \mathbf{B}' = 0$, $\rho' \neq 0$, $S' \neq 0$). For MHD models with $\nabla\cdot\mathbf{B} \neq 0$ we identify $\lambda_5$ with the divergence wave solution.

Similarly, writing

$$\mathbf{L} = (\ell_1, \ell_2, \ell_3, \ell_4, \ell_5, \ell_6, \ell_7, \ell_8) = (\ell_1, \delta\mathbf{a}^T, \delta\mathbf{b}^T, \ell_8), \tag{B 13}$$

for the left eigenvectors of the matrix $\mathbf{A}_n \equiv \mathbf{A}_c$ where $\delta\mathbf{a} = (\ell_2, \ell_3, \ell_4)^T$ and $\delta\mathbf{b} = (\ell_5, \ell_6, \ell_7)^T$, the left eigenvector equations can be written in the form

$$\tilde{u}_n\ell_1 = 0, \tag{B 14}$$

$$\tilde{u}_n\delta a_{\parallel} + (\ell_1\rho + \ell_8 a^2\rho) + \mathbf{B}_{\perp}\cdot\delta\mathbf{b}_{\perp} = 0, \tag{B 15}$$

$$\tilde{u}_n\delta\mathbf{a}_{\perp} - B_n\delta\mathbf{b}_{\perp} = 0, \tag{B 16}$$

$$\tilde{u}_n\delta b_{\parallel} - \frac{\delta\mathbf{a}\cdot\mathbf{B}}{\mu\rho} = 0, \tag{B 17}$$

$$\tilde{u}_n\delta\mathbf{b}_{\perp} - \frac{B_n}{\mu\rho}\delta\mathbf{a}_{\perp} + \frac{\delta a_{\parallel}}{\mu\rho}\mathbf{B}_{\perp} = 0, \tag{B 18}$$

$$\tilde{u}_n\ell_8 + \frac{\delta a_{\parallel}}{\rho} = 0, \tag{B 19}$$

where $\delta a_{\parallel} = \ell_2$, $\delta b_{\parallel} = \ell_5$, $\delta\mathbf{a}_{\perp} = (0, \ell_3, \ell_4)$ and $\delta\mathbf{b}_{\perp} = (0, \ell_6, \ell_7)$. Thus, the left eigenvectors $\{\mathbf{L}_s : 1 \leqslant s \leqslant 8\}$ of the matrix $\mathbf{A}_n$ are obtained by solving (B 14)-(B 19).

https://doi.org/10.1017/S0022377809990596 Published online by Cambridge University Press

We use the notation:

$$\mathbf{R}_1 = R_f^-, \quad \mathbf{R}_2 = \mathbf{R}_A^-, \quad \mathbf{R}_3 = \mathbf{R}_s^-, \quad \mathbf{R}_4 = \mathbf{R}_e,$$

$$\mathbf{R}_5 = \mathbf{R}_d, \quad \mathbf{R}_6 = \mathbf{R}_s^+, \quad \mathbf{R}_7 = \mathbf{R}_A^+, \quad \mathbf{R}_8 = \mathbf{R}_f^+, \tag{B 20}$$

where $f$, $s$, $A$, $e$, and $d$ denote the fast magnetoacoustic, slow magnetoacoustic, Alfvén, entropy, and divergence waves. The same notation is used for the left eigenvectors $\{\mathbf{L}_j : 1 \leqslant j \leqslant 8\}$.

The eigenequations (B 1)–(B 6) and (B 14)–(B 19) have solutions for the right and left eigenvectors of the form

$$\mathbf{r}^{(ma)} = \left[1, \frac{c}{\rho}\left(\mathbf{n} - \frac{b_n \mathbf{b}_\perp}{c^2 - b_n^2}\right)^T, \frac{c^2 \mathbf{B}_\perp^T}{(c^2 - b_n^2)\rho}, a^2\right]^T, \tag{B 21}$$

$$\mathbf{l}^{(ma)} = \left[0, c\left(\mathbf{n} - \frac{b_n \mathbf{b}_\perp}{c^2 - b_n^2}\right)^T, \left(\frac{b_n^2(b^2 - c^2)\mathbf{n} + c^2 b_n \mathbf{b}_\perp}{(c^2 - b_n^2)B_n}\right)^T, \frac{1}{\rho}\right], \tag{B 22}$$

where $\mathbf{b}_\perp = \mathbf{b} - b_n \mathbf{n}$ is the component of $\mathbf{b}$ perpendicular to $\mathbf{n}$ and $c$ is one of the magnetoacoustic velocities ($c = \pm c_{f,s}$), and the superscript ($ma$) denotes magnetoacoustic modes.

To obtain a well-defined set of right and left eigenvectors for the case of parallel ($\mathbf{n} \parallel \mathbf{B}$) and perpendicular ($\mathbf{n} \perp \mathbf{B}$) propagation for the MHD system with $\nabla \cdot \mathbf{B} = 0$, Roe and Balsara (1996) considered the renormalized eigenvectors:

$$\mathbf{R}^{(ma)} = k^r \mathbf{r}^{(ma)}, \quad \mathbf{L}^{(ma)} = k^l \mathbf{l}^{(ma)}, \tag{B 23}$$

such that $\mathbf{L}^{(ma)}$ and $\mathbf{R}^{(ma)}$ for the different eigenmodes form an orthonormal set. This was achieved by choosing

$$k^r k^l = \frac{\rho |c^2 - b_n^2|}{2c^2 (c_f^2 - c_s^2)} = \frac{1}{N}, \tag{B 24}$$

where $\mathbf{l}^{(ma)} \cdot \mathbf{r}^{(ma)} = N$ for the left and right eigenvectors for the same mode.

The conditions (B 24) for the fast and slow magnetoacoustic modes gives the equations (e.g., Roe and Balsara 1996)

$$k_f^r k_f^l = \frac{\rho}{2a^2}\alpha_f^2, \quad k_s^r k_s^l = \frac{\rho}{2a^2}\alpha_s^2, \tag{B 25}$$

where

$$\alpha_f = \left(\frac{a^2 - c_s^2}{c_f^2 - c_s^2}\right)^{1/2}, \quad \alpha_s = \left(\frac{c_f^2 - a^2}{c_f^2 - c_s^2}\right)^{1/2}. \tag{B 26}$$

Note that $\alpha_f$ and $\alpha_s$ satisfy the equations

$$\alpha_f^2 + \alpha_s^2 = 1, \quad \alpha_f \alpha_s = \frac{a b_\perp}{c_f^2 - c_s^2}. \tag{B 27}$$

The choices

$$k_f^r = \alpha_f, \quad k_f^l = \frac{\rho \alpha_f}{2a^2}, \quad k_s^r = \alpha_s, \quad k_s^l = \frac{\rho \alpha_s}{2a^2}, \tag{B 28}$$

https://doi.org/10.1017/S0022377809990596 Published online by Cambridge University Press

give well defined left and right eigenvectors for the fast mode eigenvectors as

$$\mathbf{R}_f^{\pm} = \left[\alpha_f, \pm\frac{1}{\rho}\left(\alpha_f c_f \mathbf{n} - \alpha_s c_s \mathrm{sgn}(b_n)\beta_\perp\right)^T, \alpha_s a\left(\frac{\mu}{\rho}\right)^{1/2}\beta_\perp^T, \alpha_f a^2\right]^T, \tag{B 29}$$

$$\mathbf{L}_f^{\pm} = \frac{1}{2}\left[0, \pm\frac{\rho}{a^2}\left(\alpha_f c_f \mathbf{n} - \alpha_s c_s \mathrm{sgn}(b_n)\beta_\perp\right)^T,\right.$$

$$\left.\frac{\rho^{1/2}}{\mu^{1/2}a^2 c_f}\left\{\mathbf{n}\left[(\alpha_s c_s b_\perp \mathrm{sgn}(b_n) - \alpha_f c_f b_n\right] + \alpha_s a c_f \beta_\perp\right\}^T, \frac{\alpha_f}{a^2}\right] \tag{B 30}$$

where

$$\beta_\perp = \frac{\mathbf{B}_\perp}{B_\perp}. \tag{B 31}$$

Similarly, the normalized, slow mode eigenvectors are

$$\mathbf{R}_s^{\pm} = \left[\alpha_s, \pm\frac{1}{\rho}\left(\alpha_s c_s \mathbf{n} + \alpha_f c_f \mathrm{sgn}(b_n)\beta_\perp\right)^T, -\alpha_f a\left(\frac{\mu}{\rho}\right)^{1/2}\beta_\perp^T, \alpha_s a^2\right]^T, \tag{B 32}$$

$$\mathbf{L}_s^{\pm} = \frac{1}{2}\left[0, \pm\frac{\rho}{a^2}\left(\alpha_s c_s \mathbf{n} + \alpha_f c_f \mathrm{sgn}(b_n)\beta_\perp\right)^T,\right.$$

$$\left.-\frac{\rho^{1/2}}{\mu^{1/2}a^2 c_s}\left\{\mathbf{n}\left(\alpha_s c_s b_n + \alpha_f c_f b_\perp \mathrm{sgn}(b_n)\right) + \alpha_f a c_s \beta_\perp\right\}^T, \frac{\alpha_s}{a^2}\right], \tag{B 33}$$

Note that the right eigenvectors $\mathbf{R}_s^{\pm}$ are well defined for the degenerate cases of parallel ($\mathbf{n} \parallel \mathbf{B}$) and perpendicular ($\mathbf{n} \perp \mathbf{B}$) propagation. However, the left eigenvectors $\mathbf{L}_s^{\pm}$ in (B 33) diverge as $B_n \to 0$, since $\ell_5 \to \infty$ as $c_s \to 0$ in this limit (i.e., the third entry in (B 33) $\parallel \mathbf{n}$ diverges).

The normalized, right and left eigenvectors for the Alfvén waves are

$$\mathbf{R}_A^{\pm} = \left(0, \mp(\mu\rho)^{-1/2}(\mathbf{n}\times\beta_\perp)^T, (\mathbf{n}\times\beta_\perp)^T, 0\right)^T, \tag{B 34}$$

$$\mathbf{L}_A^{\pm} = \frac{1}{2}\left(0, \mp(\mu\rho)^{1/2}(\mathbf{n}\times\beta_\perp)^T, (\mathbf{n}\times\beta_\perp)^T, 0\right). \tag{B 35}$$

Similarly, the right and left eigenvectors for the entropy wave are

$$\mathbf{R}_e = (1,0,0,0,0,0,0,0)^T, \tag{B 36}$$

$$\mathbf{L}_e = (1,0,0,0,0,0,0,-1/a^2). \tag{B 37}$$

The right and left eigenvectors for the divergence wave eigenmode have the form

$$\mathbf{R}_d = \left(\rho\frac{b^2}{a^2}, 0,0,0, (B_n\mathbf{n} - \mathbf{B}_\perp)^T, \rho b^2\right)^T, \tag{B 38}$$

$$\mathbf{L}_d = \frac{1}{B_n}(0,0,0,0,\mathbf{n}^T,0), \tag{B 39}$$

where we have used the fact that $\rho b^2 = B^2/\mu$. For the choices (B 38)–(B 39) for $\mathbf{R}_d$ and $\mathbf{L}_d$ we find $\mathbf{L}_e \cdot \mathbf{R}_d = 0$ and $\mathbf{L}_d \cdot \mathbf{R}_e = 0$ which is required for the entropy

https://doi.org/10.1017/S0022377809990596 Published online by Cambridge University Press

and divergence wave eigenvectors to be orthonormal. Note that there is a problem, with the normalized divergence wave solution (B 39) for the left eigenvector $\mathbf{L}_d$ for perpendicular propagation as $B_n \to 0$ ($|\mathbf{L}_d| \to \infty$ as $B_n \to 0$).

## Appendix C

In this appendix we indicate the derivation of the field line (5.21), corresponding to the simple wave solution (5.19). From (3.23) and (5.19) we obtain for the orthonormal triad (3.23):

$$\mathbf{e}_1 = (\sin\Theta_0\cos\varphi, \sin\Theta_0\sin\varphi, \cos\Theta_0),$$

$$\mathbf{e}_2 = (-\sin\varphi, \cos\varphi, 0),$$

$$\mathbf{e}_3 = (-\cos\Theta_0\cos\varphi, -\cos\Theta_0\sin\varphi, \sin\Theta_0). \tag{C 1}$$

The curvature and torsion parameters of the curve $C$ with tangent vector $\mathbf{e}_1 = \mathbf{n}(\varphi)$ ((3.24)) are

$$\kappa = \sin\Theta_0, \quad \tau = \cos\Theta_0, \tag{C 2}$$

and

$$B_1 = B_0\cos(\Theta_0 - \alpha_0), \quad B_2 = 0, \quad B_3 = B_0\sin(\Theta_0 - \alpha_0) \tag{C 3}$$

are the components of the magnetic field parallel to $\mathbf{e}_1$, $\mathbf{e}_2$, and $\mathbf{e}_3$. Using the results (C 1)–(C 3), the field line differential (3.30) reduce to

$$\frac{d\tilde{q}_2}{d\varphi} = \cos\Theta_0\tilde{q}_3 - \sin\Theta_0\frac{\varphi}{k_0}, \tag{C 4}$$

$$\frac{d\tilde{q}_3}{d\varphi} = \frac{\tan(\Theta_0 - \alpha_0)}{k_0} - \tilde{q}_2\frac{\cos\alpha_0}{\cos(\Theta_0 - \alpha_0)}. \tag{C 5}$$

Elimination of $\tilde{q}_3$ between (C 4) and (C 5) yields the differential equation

$$\frac{d^2\tilde{q}_2}{d\varphi^2} + \frac{\cos\Theta_0\cos\alpha_0}{\cos(\Theta_0 - \alpha_0)}\tilde{q}_2 = -\frac{\sin\alpha_0}{k_0\cos(\Theta_0 - \alpha_0)}. \tag{C 6}$$

Integration of (C 4)–(C 6) gives the solutions (5.22) for $\tilde{q}_2$ and $\tilde{q}_3$. Inversion of the equations

$$\tilde{q}_1 = \sin\Theta_0(\tilde{x}\cos\varphi + \tilde{y}\sin\varphi) + \tilde{z}\cos\Theta_0,$$

$$\tilde{q}_2 = \tilde{y}\cos\varphi - \tilde{x}\sin\varphi,$$

$$\tilde{q}_3 = -\cos\Theta_0(\tilde{x}\cos\varphi + \tilde{y}\sin\varphi) + \tilde{z}\sin\Theta_0, \tag{C 7}$$

to obtain $\tilde{x}$, $\tilde{y}$, and $\tilde{z}$ then yields the field line (5.21).

## References

Abramowitz, M. and Stegun, I. A. 1965 *Handbook of Mathematical Functions*. New York: Dover.

Barnes, A. 1976 On the non-existence of plane polarized large amplitude Alfvén waves. *J. Geophys. Res.* **81**(1), 281–282.

https://doi.org/10.1017/S0022377809990596 Published online by Cambridge University Press

Berger, M. and Field, G. B. 1984 The topological properties of magnetic helicity. *J. Fluid Mech.* **147**, 133–148.

Berger, M. A. and Prior, C. 2006 The writhe of open and closed curves. *J. Phys.* A.*: Math. Gen.* **39**, 8321–8348.

Bishop, R. L. 1975 There is more than one way to frame a curve. *Am. Math. Mon.* **82**, 246–251.

Boillat, G. 1970 Simple waves in N-dimensional propagation. *J. Math. Phys.* **11**, 1482–1483.

Brio, M. and Wu, C. C. 1988 An upwind differencing scheme for the equations of magnetohydrodynamics. *J. Comput. Phys.* **75**, 400–422.

Cabannes, H. 1970 *Theoretical Magnetohydrodynamics*. New York: Academic Press.

Eisenhart, L. P. 1960 *A Treatise on the Differential Geometry of Curves and Surfaces*. New York: Dover (re-publication of 1909 Edition by Ginn. and Co.).

Goriely, A. and Tabor, M. 1997 Nonlinear dynamics of filaments I: dynamical instabilities. *Physica* D **105**, 45–61.

Holm, D. D., Marsden, J. E. and Ratiu, T. S. 1998 The Euler–Lagrange equations and semiproducts with application to continuum theories. *Adv. Math.* **137**, 1–81.

Janhunen, P. 2000 A positive conservative method for magnetohydrodynamics based on HLL and Roe methods. *J. Comput. Phys.* **160**, 649–661.

Jeffrey, A. and Taniuti, T. 1964 *Nonlinear Wave Propagation with Application to Physics, and Magnetohydrodynamics*. New York: Academic Press.

Lipschutz, M. M. 1969 *Theory and Problems of Differential Geometry. Schaum's Outline Series*. New York: McGraw-Hill.

Marsden, J. E. and Ratiu, T. S. 1994 *Introduction to Mechanics and Symmetry (Texts in Applied Mathematics, 17)*. New York: Springer.

Nadjafikhah, M. and Mahdipour-Shirayeh, A. 2009 Symmetry analysis for a new form of the vortex mode equation. arXiv:0905.0175v1 [math.DG]. Differential Geometry Dynamical Systems, **11**, 144–154.

Powell, K. G., Roe, P. L., Linde, T. J., Gombosi, T. I. and De Zeeuw, D. 1999 A solution adaptive upwind scheme for ideal magnetohydrodynamics. *J. Comput. Phys.* **154**, 284–309.

Rajee, L., Eshraghi, H. and Popovych, R. O. 2008, Multi-dimensional quasi-simple waves in weakly dissipative flows. *Physica* D **237**, 405–419.

Rajee, L. and Eshraghi, H. 2009 Multi-dimensional vortex quasi-simple waves. *Physica* D **238**, 477–489.

Roe, P. L. and Balsara, D. 1996 Notes on the eigensystem of magnetohydrodynamics. *SIAM J. Appl. Math.* **56**, 57–67.

Sahihi, T., Eshraghi, H. and Mahdipour-Shirayeh, A. 2008 Multi-dimensional simple waves in fully relativistic fluids. arXiv:0811.2307v1 [physics.flu-dyn].

Sneddon, I. N. 1957 *Elements of Partial Differential Equations*. New York: McGraw-Hill.

Webb, G. M., Ratkiewicz, R., Brio, M. and Zank, G. P. 1995 Multi-dimensional MHD simple waves. In *Solar Wind*, Vol. 8 (ed. D. Winterhalter, J. T. Gosling, S. R. Habbal, W. S. Kurth and M. Neugebauer), pp. 335–338; AIP Conference Proceedings, Vol. 382. New York: AIP.

Webb, G. M., Ratkiewicz, R., Brio, M. and Zank, G. P. 1998 Multidimensional simple waves in gas dynamics. *J. Plasma Phys.* **59**, 417–460.

Webb, G. M., Pogorelov, N. V. and Zank, G. P. 2009 MHD simple waves and the divergence wave. *Solar Wind* **12**, 4, held in St. Malo France, June 21–26, 2009.